JGR Biogeosciences

RESEARCH ARTICLE
10.1029/2021JG006630

Thermohydrological Impact of Forest Disturbances on Ecosystem-Protected Permafrost

Simone Maria Stuenzi[1,2], Stefan Kruse[1], Julia Boike[1,2], Ulrike Herzschuh[1,3,4], Alexander Oehme[1,2], Luidmila A. Pestryakova[5], Sebastian Westermann[6,7], and Moritz Langer[1,2]

[1]Alfred Wegener Institute, Helmholtz Centre for Polar and Marine Research, Potsdam, Germany, [2]Geography Department, Humboldt-Universität zu Berlin, Berlin, Germany, [3]Institute of Environmental Science and Geography, University of Potsdam, Potsdam, Germany, [4]Institute of Biochemistry and Biology, University of Potsdam, Potsdam, Germany, [5]Institute of Natural Sciences, North-Eastern Federal University in Yakutsk, Yakutsk, Russia, [6]Department of Geosciences, University of Oslo, Oslo, Norway, [7]Centre for Biogeochemistry in the Anthropocene, University of Oslo, Oslo, Norway

Abstract Boreal forests cover over half of the global permafrost area and protect underlying permafrost. Boreal forest development, therefore, has an impact on permafrost evolution, especially under a warming climate. Forest disturbances and changing climate conditions cause vegetation shifts and potentially destabilize the carbon stored within the vegetation and permafrost. Disturbed permafrost-forest ecosystems can develop into a dry or swampy bush- or grasslands, shift toward broadleaf- or evergreen needleleaf-dominated forests, or recover to the pre-disturbance state. An increase in the number and intensity of fires, as well as intensified logging activities, could lead to a partial or complete ecosystem and permafrost degradation. We study the impact of forest disturbances (logging, surface, and canopy fires) on the thermal and hydrological permafrost conditions and ecosystem resilience. We use a dynamic multilayer canopy-permafrost model to simulate different scenarios at a study site in eastern Siberia. We implement expected mortality, defoliation, and ground surface changes and analyze the interplay between forest recovery and permafrost. We find that forest loss induces soil drying of up to 44%, leading to lower active layer thicknesses and abrupt or steady decline of a larch forest, depending on disturbance intensity. Only after surface fires, the most common disturbances, inducing low mortality rates, forests can recover and overpass pre-disturbance leaf area index values. We find that the trajectory of larch forests after surface fires is dependent on the precipitation conditions in the years after the disturbance. Dryer years can drastically change the direction of the larch forest development within the studied period.

Plain Language Summary Boreal forests of eastern Siberia, cover more than half of the global permafrost area and insulate the underlying frozen ground. The development of the forest cover is important for the state and evolution of permafrost. Forest disturbances such as fires or droughts and climate change can cause changes in this ecosystem. Potentially such shifts can destabilize the carbon stored within the vegetation and permafrost. Disturbed permafrost-forest ecosystems can develop into the dry or swampy bush- or grasslands, shift toward different forest types, or recover. An increase in the number and intensity of fires, as well as intensified logging, could lead to partial or complete permafrost degradation. We study the interactions between forest disturbances, permafrost, and forests. We use a forest-permafrost model and simulate disturbances at a study site in eastern Siberia. We implement mortality, defoliation, and ground surface changes of different disturbances. We then analyze the forest recovery's impact on the permafrost underneath. We find that forest loss can cause soil drying and abrupt or steady decline of forests, depending on the intensity of the disturbance. Only after a surface fire, which has low mortality rates and is the most common disturbance, forests can successfully recover.

Key Points:

- We demonstrate a dynamic forest-permafrost model to investigate the interplay between boreal larch forest, permafrost, and disturbances
- Forest loss induces soil drying which leads to lower active layer thicknesses and abrupt or steady decline of larch forest cover
- Trajectory of larch forests after surface fires is dependent on the post-disturbance precipitation conditions

Correspondence to:
S. M. Stuenzi,
simone.stuenzi@awi.de

Citation:
Stuenzi, S. M., Kruse, S., Boike, J., Herzschuh, U., Oehme, A., Pestryakova, L. A., et al. (2022). Thermohydrological impact of forest disturbances on ecosystem-protected permafrost. *Journal of Geophysical Research: Biogeosciences*, *127*, e2021JG006630. https://doi.org/10.1029/2021JG006630

Received 15 SEP 2021
Accepted 20 APR 2022

Author Contributions:

Conceptualization: Simone Maria Stuenzi, Moritz Langer
Data curation: Simone Maria Stuenzi
Formal analysis: Simone Maria Stuenzi
Funding acquisition: Julia Boike, Ulrike Herzschuh, Moritz Langer
Investigation: Simone Maria Stuenzi, Moritz Langer
Methodology: Simone Maria Stuenzi, Stefan Kruse
Project Administration: Julia Boike, Ulrike Herzschuh, Luidmila A. Pestryakova, Moritz Langer
Resources: Simone Maria Stuenzi, Alexander Oehme, Luidmila A. Pestryakova, Moritz Langer
Software: Simone Maria Stuenzi, Stefan Kruse, Sebastian Westermann, Moritz Langer

1. Introduction

Boreal forests hold more than one-third of global terrestrial carbon and cover about 55% of the total global permafrost area (Helbig et al., 2016). The forest cover efficiently insulates the underlying, ecosystem-protected permafrost (Chang et al., 2015) and therefore plays an important role in the development of boreal regions and the stability of permafrost in a warming climate. Despite little human interference and due to extreme climate conditions such as winter temperatures below −50° C and low precipitation, the biome is highly sensitive to climatic

Supervision: Stefan Kruse, Julia Boike, Ulrike Herzschuh, Luidmila A. Pestryakova, Moritz Langer
Validation: Simone Maria Stuenzi
Visualization: Simone Maria Stuenzi
Writing – original draft: Simone Maria Stuenzi
Writing – review & editing: Simone Maria Stuenzi, Julia Boike, Alexander Oehme, Sebastian Westermann, Moritz Langer

changes and thus prone to vegetation shifts (Mamet et al., 2019; Pearson et al., 2013). While most boreal forests are dominated by evergreen needleleaf taxa, large forested regions in eastern Siberia, which make up around 20% of the global boreal forest cover, are larch (deciduous needleleaf) dominated. The larch forests foster a unique interplay between the forest cover, the underlying permafrost, and the active layer depth (Kajimoto, 2010; Peng et al., 2020; Tanaka et al., 2008; Zhang et al., 2011), disturbances (Rogers et al., 2015), and climate, and thereby inhibit the invasion of late-successional evergreen taxa (V. Kharuk et al., 2007). Recently, permafrost destabilization and vegetation shifts have become visible at many locations throughout the vast ecosystem-protected permafrost region (Ulrich et al., 2017). Often, the observed permafrost dynamics are related to anthropogenic deforestation, fires, and climate change-related forest dynamics, which bring this tightly coupled ecosystem out of balance but the exact processes and thresholds are poorly studied.

Forest composition and density exert a strong control on permafrost stability (Chasmer et al., 2011; Fisher et al., 2016; Stuenzi, Boike, Cable, et al., 2021; Yi et al., 2007) and a direct feedback mechanism, namely the thermal and hydrological conditions of the ground determine the temporal ecosystem evolution and the state of the vegetation cover (Bonan et al., 1992; Carpino et al., 2018; Loranty et al., 2018). Anthropogenically-caused disturbances and changing climate conditions are leading to shifts in this ecosystem (Baltzer et al., 2014). This could potentially destabilize the carbon stored within the vegetation and permafrost (Romanovsky et al., 2017). Disturbed permafrost-forest ecosystems can develop into the dry or swampy bush- or grasslands (X. Y. Jin et al., 2020), the shift toward broadleaf- or evergreen needleleaf-dominated forests (Rogers et al., 2015; Takahashi, 2006), or recover to the pre-disturbance state. An increase in the number and intensity of fires, and the lengthening of the fire season (Holloway et al., 2020; Narita et al., 2020), as well as intensified logging activities, could lead to partial or complete permafrost degradation and vegetation shifts away from deciduous-dominated forest stands (V. I. Kharuk et al., 2019). Especially permafrost at the southern margin might not remain resilient under a warming climate because of its dependence on ecosystem protection (Yershov, 2004). While larch growth increments and a positive gross primary production suggest higher carbon sequestration in the future (V. I. Kharuk et al., 2019), an increase in fires and carbon emissions might convert the vast larch forest into a carbon source, especially in years of extreme fires (V. I. Kharuk et al., 2021).

Previous modeling set-ups have coupled dynamic vegetation to permafrost models to study forest development and different components such as fire disturbances, topology, or the impact of greenhouse gas scenarios. Sato et al. (2010) (SEIB-DGVM) have simulated post-fire successional patterns at the Spasskaya pad without specifically incorporating permafrost dynamics and the impact of forest change on permafrost. Recently, Sato et al. (2020) have used an updated model version to study topographic control on soil-water relocation and over-wet-kill of larch trees. Furthermore, Zhang et al. (2011) studied the interactions between permafrost and forest biomass under current and future climate scenarios and have described larch-permafrost systems as a tightly-coupled ecosystem. SibClim has additionally been used to simulate vegetation shifts across eastern Siberia (Tchebakova et al., 2009) and Zhang et al. (2009) used FAREAST to model the responses of eastern Eurasian forests to climatic change to understand the compositional and structural sensitivity at several locations. Furthermore, an updated version of FAREAST called UVAFME (Foster et al., 2019) has been used to simulate Russian forest dynamics under different greenhouse gas emission scenarios (Shuman et al., 2014) and along with a fire disturbance module to track mortality at tree-species and -size level, and biomass and species dynamics (Shuman et al., 2017). This study found that larch remained dominant after a specific fire disturbance and under an altered climate scenario, and concluded that complex competition at the species level is important in evaluating forest response to fire and climate. In a study on the distribution of vegetation productivity trends, wildfires, and near-surface soil carbon, Loranty et al. (2016) have found positive vegetation productivity trends in continuous permafrost and less positive and negative trends in discontinuous. These results indicate that productivity trends (greening or browning) might be directly linked to permafrost distribution. Takahashi (2006) used artificial fire at Spasskaya pad to study fire dynamics and succession and described the common forest dynamic patterns leading to regeneration or degradation of larch forests. Petrov et al. (2022) studied ground temperature and active layer thickness observations at the same site and found that the permafrost progressively restabilized following forest fires. Moreover, Yoshikawa et al. (2002) found that heat transfer through conduction was not significant during a fire and that active layer thickening depends heavily on the thickness of the remaining organic soil layer. In Canadian boreal forest areas, Rey et al. (2020) have found that the pre-disturbance soil conditions are key factors controlling the thawing and talik formation processes, and wildfire initiated talik-development is already substantial. Finally, Alexander et al. (2012) evaluated pre- and post-fire carbon accumulation patterns in Siberian larch stand throughout the

different successional stages. They found that increasing fire frequencies without altered stand densities could likely lead to declined landscape-level carbon storage. If, on the other hand, larch densities increase after fires the larger above-ground carbon pools could compensate for the shorter successional cycle. In summary, former studies on stand-replacing or surface fires and other disturbances in eastern Siberia have focused on their implications on the carbon budget (Alexander et al., 2012; Schulze et al., 2012; Soja et al., 2004), their potential impact through surface albedo change and related surface radiative forcing (Chen et al., 2018; Chen & Loboda, 2018; Stuenzi & Schaepman Strub, 2020), or the following successional patterns and species compositions (Takahashi, 2006; Shuman et al., 2014, 2017). While all of these studies have greatly improved our understanding of the underlying mechanisms in the tightly coupled permafrost larch ecosystems of eastern Siberia, they often lack the incorporation of a physically-based representation of the heat and water exchange between the canopy and the ground. Further work is therefore needed to identify the post-disturbance response of permafrost (Holloway et al., 2020), and the related interplay between the living forest and the permafrost (Li et al., 2021).

We apply a dynamic vegetation-permafrost model (Kruse, Stuenzi, Boike, et al., 2022), based on the one-dimensional permafrost land surface model, CryoGrid (Westermann et al., 2016), and the individual-based and spatially explicit larch forest model LAVESI (Kruse et al., 2016). The permafrost model was adapted for use in boreal forest ecosystems (Stuenzi, Boike, Cable, et al., 2021; Stuenzi, Boike, Gädeke, et al., 2021) by adding a state-of-the-art multilayer vegetation model (CLM-ml v0, originally developed for the Community Land Model (CLM) by Bonan et al. (2018). The resulting coupled model (CryoGrid-Vegetation) is a highly detailed land surface model capable of reproducing the heat and water transfer through a dynamically evolving forest canopy with its root zone essentially controlled by permafrost. The model has previously been used to study the thermo-hydrological impact of different forest cover densities and compositions on the underlying permafrost. Here, the use of this model with the larch forest simulator described in detail in Kruse, Stuenzi, Boike, et al. (2022) forms a dynamic vegetation-permafrost model which can reproduce the complex interplay between larch forests and the dynamically changing soil conditions linked to permafrost. We reconstruct vegetation disturbance scenarios (surface and canopy fires, and logging) and simulate such scenarios at a specific, well-described site in central Yakutia. We study the interplay between forest disturbances, larch recovery, and the thermo-hydrological ecosystem factors. We shift the focus from vegetation succession toward the assessment of the impact different disturbances have on the hydro-thermal regime of permafrost and its feedback to the deciduous larch forest on a mid-term temporal scale (29 years, until 2050). We investigate the complex interplay between forest disturbances, permafrost conditions, and changing ecological factors which control larch forest stand recovery and permafrost dynamics to understand how certain disturbances, in combination with projected changing climatic conditions, can push this tightly coupled system out of balance.

The main objectives of this study are

1. to demonstrate the capabilities of a coupled, dynamic multilayer forest – permafrost model to simulate the interplay within the highly sensitive system formed by dynamic boreal larch forest and permafrost
2. to investigate which disturbances and intensities occur in our study region and under which climatic circumstances they trigger the tightly coupled system to get out of balance, and
3. to study when and how the thermal and hydrological conditions of the underlying permafrost and the larch forest cover itself can reach a new state

2. Materials and Methods

2.1. Study Region

We used a site previously used for model validation at the southern margin of continuous permafrost to evaluate the permafrost's resilience toward forest disturbance scenarios. Our study site Spasskaya pad (SPA) is located at N 62.14°, E 129.37°, about 20 km north of Yakutsk, on the western side of the central Lena river, at an elevation of 237 m a.s.l (Maximov et al., 2019). The region is underlain by continuous permafrost and the majority of the forested area is dominated by the deciduous species Dahurian larch (*Larix gemelinii*, 89–90%), while 6% is covered by Scots pine (*Pinus sylvestris*), which prefer sandier soils. The rest of the area is vegetated by willow birch, a successful early-successor after forest disturbances. Especially after disturbances, deciduous species such as Alnus or Betula can also grow in the forest stands. Ground is covered by dense understory vegetation

such as *Vaccinium vitis-idaea* growing 0.05 m tall. Sugimoto et al. (2002) report a stem density of 836 stems per ha and a basal area of 27.12 m^2ha^{-1} for larch. Leaf-out of deciduous larch taxa has been observed in mid-May, with a growing period until late August. The topography is quite flat with an incline of 1.6° toward the north-east. Mean annual air temperature reaches −5.97° C, with an average of −12.7° C during the snow-covered and 13.7° C during the snow-free periods. Liquid precipitation adds up to around 170 mm and solid precipitation to 84 mm (Simmons et al., 2007). In very dry and harsh conditions, larch trees restrict growth and photosynthetic capacity, by using water efficiently through stomata closure regulation (Baldocchi et al., 2004). Additionally, they use snow and ground ice melt water from the seasonally thawing permafrost (Kelliher et al., 1998). Therefore their physiological conditions are closely linked to the soil moisture dynamics. At Spasskaya pad active layer thickness is typically 1.0–1.4 m under larch forest. The ecological optimum of Siberian larch is far from the cold climate and frozen soils but in the milder climatic conditions they are out-competed by stronger competitors such as evergreen spruce or pine, and thus pushed out to the less favorable sites, such as the north (Abaimov et al., 1998). Their main rooting mass (80%) is concentrated in the upper, 0.3 m deep soil layer (Stuenzi, Boike, Cable, et al., 2021; Stuenzi, Boike, Gädeke, et al., 2021). On the warmed up and well drained plots, the roots of *Larix gemelinii* can penetrate to the depth of 0.8–1 m. Under optimal ecological conditions the tallest trees of *Larix gemelinii* can reach the height of 35–40 m (Abaimov et al., 1998).

2.2. Model and Setup Description

We apply a detailed permafrost-dynamic vegetation model based on CryoGrid-Vegetation described in (Stuenzi, Boike, Cable, et al., 2021; Stuenzi, Boike, Gädeke, et al., 2021), and LAVESI, an individual-based larch vegetation simulator, originally described in Kruse et al. (2016).

2.2.1. CryoGrid-Vegetation

The permafrost model is based on a one-dimensional, numerical land surface model that simulates the thermo-hydrological regime of permafrost ground (Nitzbon et al., 2019). The thermo-hydrological regime is simulated by numerically solving the one-dimensional heat equation with groundwater phase change. We used a modified nonisothermal Richards equation to solve flow in freezing soil based on the parameterization in Painter and Karra (2014). This relationship for phase partitioning of water in frozen soil shows improved performance for unsaturated ground conditions by smoothing the thermodynamically derived relationship to eliminate jump discontinuity at freezing. The exchange of sensible and latent heat, radiation, evaporation, and condensation at the ground surface are simulated with a surface energy balance scheme based on atmospheric stability functions. The model simulates the evolution of the snow cover using a detailed parameterization first implemented in Zweigel et al. (2021) and based on the CROCUS snow cover scheme (Vionnet et al., 2012).

This model has previously been extended by a multilayer canopy module for use in boreal permafrost regions developed by Bonan et al. (2014). The multilayer canopy model provides a comprehensive parameterization of fluxes from the ground, through the canopy up to the roughness sublayer. In an iterative manner, photosynthesis, leaf water potential, stomatal conductance, leaf temperature and leaf fluxes are calculated. This improves model performance in terms of capturing the stomatal conductance and canopy physiology, nighttime friction velocity and the diurnal radiative temperature cycle, and sensible heat flux (Bonan et al., 2014, 2018). The within-canopy wind profile is calculated using above- and within-canopy coupling with a roughness sublayer (RSL) parameterization (see Bonan et al. [2018] for further detail). The canopy model has been coupled to CryoGrid by replacing its standard surface energy balance scheme while soil state variables are passed back to the forest module (see Stuenzi, Boike, Cable, et al. [2021] and Stuenzi, Boike, Gädeke, et al. [2021] for additional model details). The vegetation module forms the upper boundary layer of the coupled model and replaces the surface energy balance equation used for common CryoGrid representations. CryoGrid operates at a 1D spatial resolution and a 5-min time-step. The model does not account for lateral water fluxes or topography. These fluxes are extremely small at this dry, flat, and homogeneous study site and therefore do not play an important role in the permafrost hydrology here. The multilayer canopy model requires a minimum LAI of 0.7 m^2m^{-2} and a minimum tree height of 1 m to set up a full canopy structure with multiple canopy layers. These layers are required for the successful simulation of the radiative transfer through the canopy and for the roughness

sublayer scheme. This scheme is based on the Harman et al. (2008) roughness sublayer theory which was developed for dense forests. Therefore, a forest cover below this threshold is considered forest cover free.

2.2.2. LAVESI

LAVESI is an individual-based, spatially-explicit, and pattern-oriented model that simulates larch stand dynamics and was originally described in Kruse et al. (2016). The relevant processes (growth, seed production and dispersal, establishment and mortality) are incorporated and adjusted to observation data gained from field surveys and literature. LAVESI simulates the forest cover dynamics at a yearly temporal resolution and at two hierarchical levels, the simulation area, which is characterized by a specific biotic and abiotic environment, and by individual trees and seeds. The trees and seeds are exactly positioned by x,y coordinates. Here, we used the updated LAVESI version described in detail in Kruse, Stuenzi, and Gloy (2022). One simulation step equals 1 year and competition, growth, seed production, and dispersal, establishment, and mortality are invoked consecutively. For resource competition, basal diameters of the individual trees are used to calculate the competition strength between neighboring trees. Based on competition and the maximum possible tree growth each year, the growth of every individual tree is calculated. The seeds are dispersed from parent trees at a set rate and with decreasing probability for longer distances. Seed production of mature trees depends on weather, competition, and tree size, and the seeds on the ground germinate depending on weather conditions. Finally, seeds and trees are removed ("die") at a specific mortality rate based on long-term mean weather values, a drought index, the surrounding tree density, tree age, and size. The model was implemented in C++ using standard template libraries and compilations. Further LAVESI parameters are provided in the original descriptions in Kruse et al. (2016, 2018) and Kruse, Stuenzi, Boike, et al. (2022). Newly introduced parameters are provided in Table A2.

2.2.3. Model Description and Setup

To dynamically update the vegetation cover and therefore allow for the simulation of disturbance scenarios we applied the coupled *Larix Vegetation Simulator* (LAVESI) permafrost energy transfer model (CryoGrid-Vegetation) described in Kruse, Stuenzi, Boike, et al. (2022). This coupled model can simulate the energy- and water exchange processes in permafrost-larch environments including mortality after different disturbance scenarios and reestablishment of larch taxa. LAVESI, with a yearly time step, served as the host and called individual CryoGrid-Vegetation instances. Here, we used a total LAVESI plot size of 1250 × 1250 m. This simulated forest patch in LAVESI is coupled to the one-dimensional CryoGrid-Vegetation model by separating the study plot area into three sub-areas for which individual CryoGrid-Vegetation instances were run. The spatial variability of the forest cover is, thus, explicitly represented by an ensemble of three parallel CryoGrid instances (sub-areas). Topography or lateral water fluxes between these sub-areas are not represented. The stand specific state variables are leaf area index (LAI), stem area index (SAI), plant area index (PAI), litter layer height, organic soil layer, ground surface albedo and soil moisture content. These key variables representing the three sub-areas are provided to CryoGrid by LAVESI and based on them, individual CryoGrid-Vegetation simulations are started in parallel via a system call. In exchange, LAVESI receives the yearly total plant available groundwater in percent (PAW), and the maximum active layer thickness (ALT). The output generated by the three CryoGrid-Vegetation instances is extrapolated back to the original resolution of the environmental grid used in LAVESI (see Kruse, Stuenzi, Boike, et al. [2022] for additional model details). The optimum plant available water levels for growth for the simulated *Larix gmelinii* tree species is between 21.1% and 40% (Sato et al., 2010). When actual levels fall below 15% or exceed 60%, trees get a growth penalty of 10%.

2.3. Forest Disturbance Scenarios and Model Simulations

We used this coupled, dynamic vegetation-permafrost model to study permafrost conditions under natural, disturbance-driven, and climate change-induced forest cover dynamics.

2.3.1. Forest Disturbance Scenarios

In the following, different disturbances occurring in boreal forests are introduced. Based on impact size and frequency we focus on two main disturbance classes: forestry and fire (see Figure 1). We further specify three

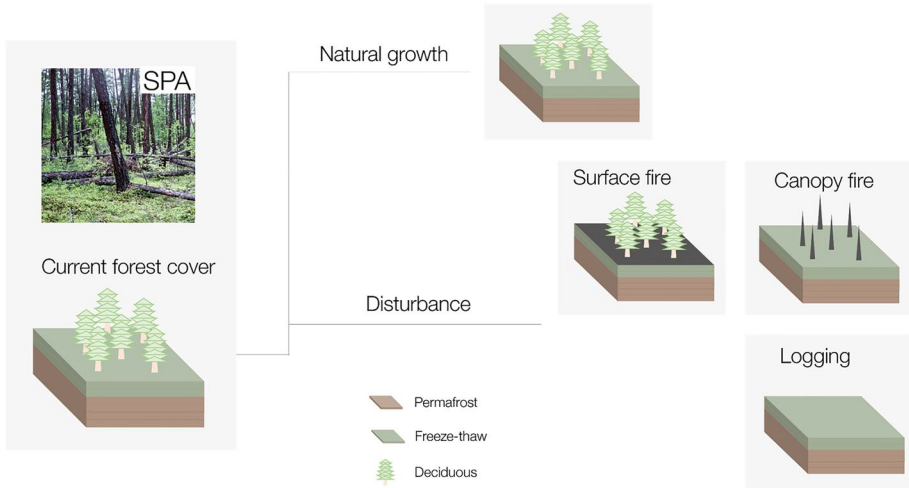

Figure 1. Left: Photograph and schematic illustration of the current forest cover at the study site, SPA. Right: Schematic illustration of the different development trajectories and their impact on the ecosystem including natural growth without any external disruptions, and the main disturbances, logging, and fires (surface and canopy).

different intensity classes based on literature values of mortality and defoliation, organic and litter layer damage, and a change in ground surface albedo (Averensky et al., 2010; Kirichenko et al., 2009; Narita et al., 2020; Shvidenko & Nilsson, 2000).

A relevant factor in the development of boreal forests is the importance of logging. In Yakutia, the forestry industry started recovering around 2000 after a sharp reduction between 1990 and 2000. In 2015, 1,000,000 m^3 of wood have been sold (Narita et al., 2020). Low-developed transport infrastructure and remoteness of the foreign and domestic markets hinder large-scale timber production in the Sakha republic, which is therefore not of importance to the republic's economy and only accounts for roughly 1% of the exports. Accordingly, 97% of the harvested wood goes to the domestic market (Oleg Tomshin, personal communication, 31 October 2017). Based on this, it is assumed that logging does not account for a substantial part of the region's forest loss, but accessible forest stands in the vicinity of settlements and roads are prone to small- and large scale deforestation. We divide logging into three classes of intensity from a thinning where a quarter of trees are removed to a clear cut with 100% tree removal.

The most prominent disturbance in terms of area size and occurrences are forest fires (Giglio et al., 2003). In Yakutia, the annual average fire area between 2015 and 2018 was estimated to 10,405 km^2 (Narita et al., 2020). Forest fires are the largest cause of forest loss or forest destruction in eastern Siberia. Fires are caused by dry thunderstorms, and human factors such as agricultural burning. The causes of ignition are hard to backtrack but it is assumed that around 70% of fires are anthropogenic (Takahashi, 2006). Larch is generally well adapted to wildfires and protected by its thick bark (Wirth, 2005). Additionally, larch drop low-hanging branches which limit the chances of a fire spreading into the canopy (Wirth, 2005). Finally, the low canopy closure additionally lowers the chance of high severity canopy fires (V. I. Kharuk et al., 2011; Schulze et al., 2012). There are different types of fires, which are classified into two categories, surface and canopy fires. Most common are surface fires which are quick and result in low energy output. They do not necessarily harm living trees, and are commonly rather nondestructive with mortality rates from 12% to 50% (V. I. Kharuk et al., 2010; Shvidenko & Nilsson, 2000). Nevertheless they have a large effect on the forest development especially by reducing the organic and litter layers and impacting the surface and the ground surface albedo (Ponomarev et al., 2016). In a study using artificial fires at SPA, the canopy photosynthesis was not affected the year after a surface fire, but the mortality was increased in the following years (Takahashi, 2006). Tree die-back is increased for up to 5 years and mortality for up to 10 years (Shvidenko & Nilsson, 2000). Less common but more destructive are canopy fires, consuming most trees, including their crowns, and leading to mortality rates between 60% and 100%. The variation in the mortality caused by forest fires is very high (Shvidenko & Nilsson, 2000). Therefore, we defined 6 different categories, making a distinction between surface and canopy fires and intensities. A low intensity surface fire

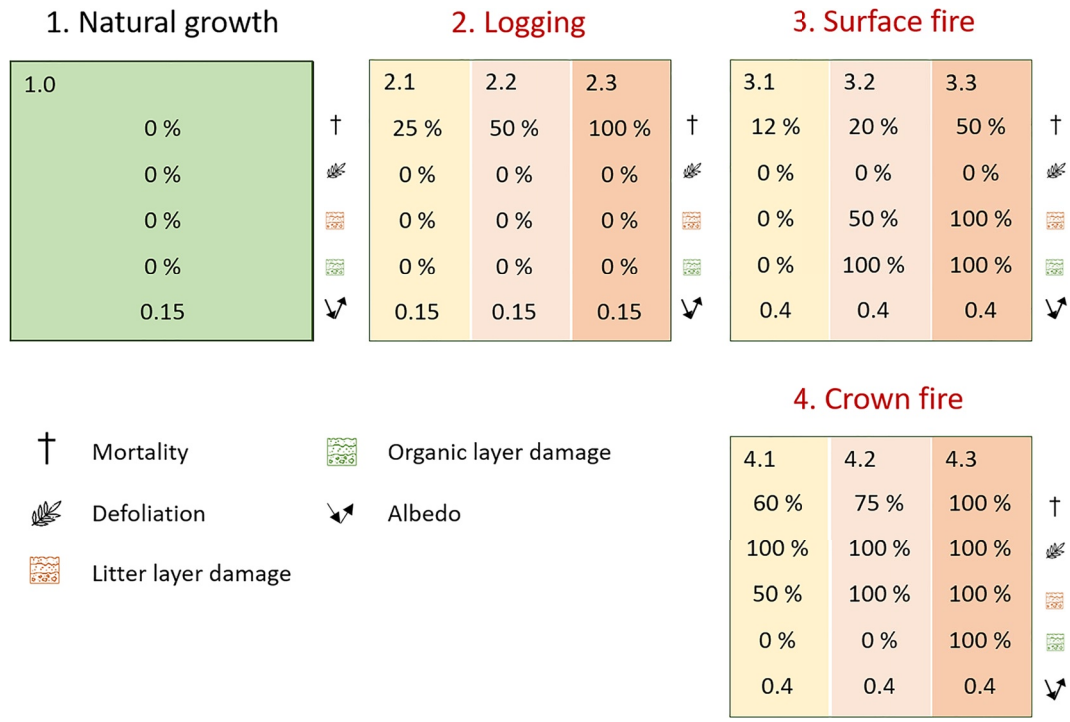

Figure 2. Schematic of the four simulations with the respective values for mortality, defoliation, change in litter layer height, the existence of an organic layer and ground surface albedo change. Left: Undisturbed, natural vegetation growth. Middle/right: Implementation of the three disturbance scenarios, logging, surface fire, crown fire.

causes the forest to go through natural thinning, where the smallest and weakest, or pre-damaged trees die. After a medium intensity fire the seeds of some trees survive and can trigger the regeneration of the coniferous forest. After a high-intensity crown fire, the trees are killed and dry out, resulting in the accumulation of partly burned material on the ground, and widespread degradation of the forest (Shvidenko & Nilsson, 2000; Takahashi, 2006). Injuries to the crown foliage can be differentiated into crown consumption (heat death and consumption of foliage, buds, branches and flowers), crown kill (heat death of foliage, buds, branches, and flowers), or crown scorch (heat death of foliage only, surviving bud; Varner et al. [2021]). Following heat death, the needles will eventually fall off while the buds can survive. Depending on the injuries to the foliage as well as on the conditions of the roots and bark the tree can still survive a canopy fire with or without impairment of physiological activity or tree growth (e.g., Lodge et al. (2018)). Therefore, the canopy fire scenarios lead to the defoliation of all trees. The long-term effects of fire on the soil thermal regime are poorly understood. The organic layer in deciduous forests decays more quickly than in evergreen forests and it is speculated that the organic layer is fully reestablished after 10–25 years (Bonan & Shugart, 1989; Foster et al., 2019). Wildfires elevate the overall surface albedo of these forested areas through different mechanisms such as the exposure of the previously shielded forest floor and an elevated snow season albedo due to a (partly) missing forest canopy. Additionally, the dominance of early-succession species such as birch or aspen, and the regrowth of light early-successional ground vegetation also lead to a higher ground surface albedo (Randerson et al., 2006; Stuenzi & Schaepman Strub, 2020). Y. Jin et al. (2012) found that the higher spring albedo and large albedo increases in areas that had burned more severely were sustained for at least 7 years after fire.

2.3.2. Scenario-Based Model Parameters

We ran model simulations for the above disturbance scenarios under two different climate scenarios at a typical, larch-dominated forest patch at our study site SPA. Additionally, we ran reference simulations without any disturbances (see Figure 2). Based on the most common disturbances and their impact on the vegetation in terms of increased mortality or defoliation, we simulated a variety of forest stand scenarios to understand threshold

values in the forest-permafrost dynamics. The different scenarios represented by three intensities each are run as three parallel point simulations. The simulations do not consider border effects but rather simulate three extreme cases of low, medium, or high intensities. The choices in parameters for mortality, defoliation, organic and litter layer damage, and the change in ground surface albedo were based on measured ground data in as many cases as possible and were collected from a variety of studies (Averensky et al., 2010; Kirichenko et al., 2009; Narita et al., 2020; Shvidenko & Nilsson, 2000). We implemented the disturbance scenarios in 2020. Tables A1, A3, and A5 summarize the ground and vegetation parameter setups. Table A4 summarizes all constants used.

The disturbance scenarios were implemented in LAVESI at the export stage where data is compiled for CryoGrid. For all scenarios we split the total simulated area into three equally-sized subareas to represent the three scenario intensities (see Figure 2). For each, LAVESI aggregates the necessary output to call CryoGrid. Leaf area index (LAI), stem area index (SAI), the 75-percentile tree height, and litter layer height are exported. Additionally, the static variables (albedo and organic content) are set based on literature values as detailed in the following and visualized in Figure 2. In the natural growth scenario there is no increased mortality or defoliation, and no litter layer damage. Ground surface albedo is set to the standard value of 0.15, the organic layer is undamaged. In the logging scenario, trees are removed randomly with a probability of 25% (subarea 2.1), 50% (2.2), and 100% (2.3). There is no additional defoliation and no litter layer damage, the ground surface albedo is at the standard value of 0.15, and the organic layer is undamaged. In the surface fire scenario, trees are removed randomly with a probability of 12% (3.1), 20% (3.2), and 50% (3.3; Shvidenko & Nilsson, 2000). Ground surface albedo is set to the increased value of 0.4 for a total of 7 years (Y. Jin et al., 2012; Randerson et al., 2006). The organic layer is reduced to 10% (3.2), and completely removed (3.3), growing back linearly within 10 years (Bonan & Shugart, 1989). For the crown fire scenario, trees are removed randomly with a probability of 60% (4.1), 75% (4.2), and 100% (4.3; Shvidenko & Nilsson, 2000). Trees are additionally completely defoliated following Varner et al. (2021). Ground surface albedo is set to 0.4, coming back to the standard value of 0.15 after 7 years (Y. Jin et al., 2012). The organic layer thickness is reduced to 10% (4.1) and completely removed in the other subareas (4.2 and 4.3), growing back linearly within 10 years (Bonan & Shugart, 1989).

The different time-steps (yearly for LAVESI, 5-min for CryoGrid) of the two models require differing spin-up periods. LAVESI spin-up is 2015 years to achieve larch forest stands that are in equilibrium with climate. For the year 2010 forest state variables are first provided to CryoGrid-Vegetation. Following previous studies (Stuenzi, Boike, Cable, et al., 2021), CryoGrid-Vegetation only requires a spin-up of 5 years (2010–2014) to bring the thermo-hydrological state of the active layer into dynamic equilibrium. For the year 2015 ALT and PAW values are delivered to LAVESI. The first year of coupling is therefore 2015 when both models have reached their equilibrium states.

2.3.3. Meteorological Forcing Data

The meteorological forcing data used by CryoGrid (air temperature, air pressure, wind speed, relative humidity, solid and liquid precipitation, incoming long- and shortwave radiation, and cloud cover) are obtained from ERA-5 (ECMWF Reanalysis) extracted for the site (N 62.14°, E 129.37°) at a 1-hourly time-step (Hersbach et al., 2018). Scenario data from the MPI-ESM1.2-HR model of the Max Planck Institute for Meteorology (Müller et al., 2018) was then applied as 6-year monthly mean anomalies, relative to the reference period 2015–2020, to the ERA5 data to generate forcing data for the projected timespan 2021–2050 and the two climate change scenarios (SSP - Shared Socioeconomic Pathways: SSP1-2.6 and SSP5-8.5; Koven et al. [2015]). The MPI-ESM1.2-HR (with a spatial resolution of 0.94° EW × 0.94° NS or approx. 100 km) model grid was interpolated to fit the ERA-5 grid. Temperature threshold for snow versus rain is 0° C, and the minimum wind speed is set to $0.5^{m/s}$. From the same data, the necessary forcing data for LAVESI was aggregated. LAVESI requires a monthly mean temperature of the coldest (January) and warmest (July) months, precipitation series, and 6-hourly wind speed and direction. Prior to the ERA-5 period (0–1978) we used the monthly Climate Research Unit data set CRU TS 2.23 available at a 0.5° resolution (Harris et al., 2020) to force LAVESI. We performed model simulations until 2050 under two projected climate change scenarios (SSP - Shared Socioeconomic Pathways) SSP1-2.6 (atmospheric CO_2 around 420 parts per million (ppm) and global temperatures 1.3–1.9° C above pre-industrial levels by 2100), and SSP5-8.5 (atmospheric CO_2 around 935 parts per million (ppm) and global temperatures 4–6.1° C above pre-industrial levels by 2100).

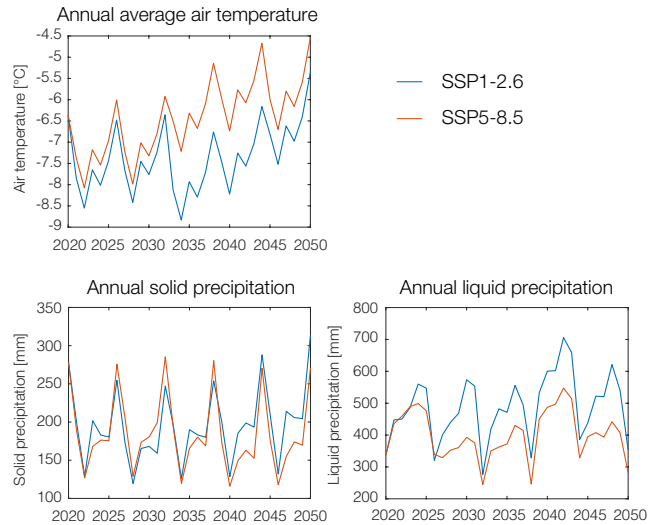

Figure 3. Comparison of the climate data forcing of SSP1-2.6 (blue) and SSP5-8.5 (red) for annual average air temperature, annual summed liquid and solid precipitation for the period 2020–2050.

3. Results

We first discuss the model verification for the study site and give an overview of the projected climatic changes. We then report on the forest stand developments under natural and disturbance-driven conditions. Lastly, we focus on the post-disturbance hydrological and thermal regimes of the underlying permafrost.

3.1. Model Verification

The multilayer canopy-permafrost model CryoGrid-Vegetation has previously been validated against ground surface temperature, the above- and below-canopy surface energy balances, snow depth, conductive heat flux, precipitation, and temperature measurements for SPA acquired through the AsiaFlux network (AsiaFlux, 2017). The analysis revealed a satisfactory agreement between modeled and measured components of the surface energy balance below and above the canopy (more details in Stuenzi, Boike, Cable, et al. [2021]). Site-specific LAVESI model verification for SPA was performed by comparing modeled and field-based stand density, leaf area index, and tree height values. The initial parameters set in the current LAVESI model version simulated a larch forest similar to the present stands at SPA. Modeled summer LAI reached 3.56 m^2m^{-2} after model spin-up which compares very well with the measured LAI value of 3.66 m^2m^{-2} at SPA (Ohta et al., 2001; Sugimoto et al., 2002). According to a field study at Spasskaya pad (Ohta et al., 2001), the stand density of the dominant tree species *Larix gmelinii* is 840 trees per hectare and 836 trees per hectare Sugimoto et al. (2002). Modeled larch stand density here is 801 trees per hectare in 2014 and 817 trees per hectare in 2019. The average tree height at Spasskaya pad has been reported as 18 m for a mature larch stand (Ohta et al., 2001) and 7.6 m for a younger larch stand with a mean stand height of 17.3 m for the 10 tallest trees (Tanaka et al., 2008). The simulated average tree height in LAVESI is 10.1 m in 2015 and 10.2 m in 2019 (see Figure C2). These average stand heights are skewed toward small saplings, which are immediately counted as trees in LAVESI but were most likely not included in the field surveys. Previous to the coupling, LAVESI overestimated ALT by up to 10% (0.01 m). Additionally, the plant's available water was overestimated by 12%. Across all simulations conducted here, average LAI before coupling in 2015 is 3.56, m^2m^{-2} (SD: 0.4) and after coupling in 2019 it is 3.6, m^2m^{-2} (SD: 0.4). Average tree height in 2015 is 10.14 m (SD: 0.06) and in 2019, after coupling it is 10.19 m (SD: 0.05). Furthermore, the modeled values of ALT: 0.96–0.99 m (±0.1) and PAW: 17.03–17.24% (±1–1.3)) show a good agreement with measured values for SPA presented in Sato et al. (2016) where ALT under larch forest was 1.04 m and soil wetness was 20.7% in the top 0.5 m.

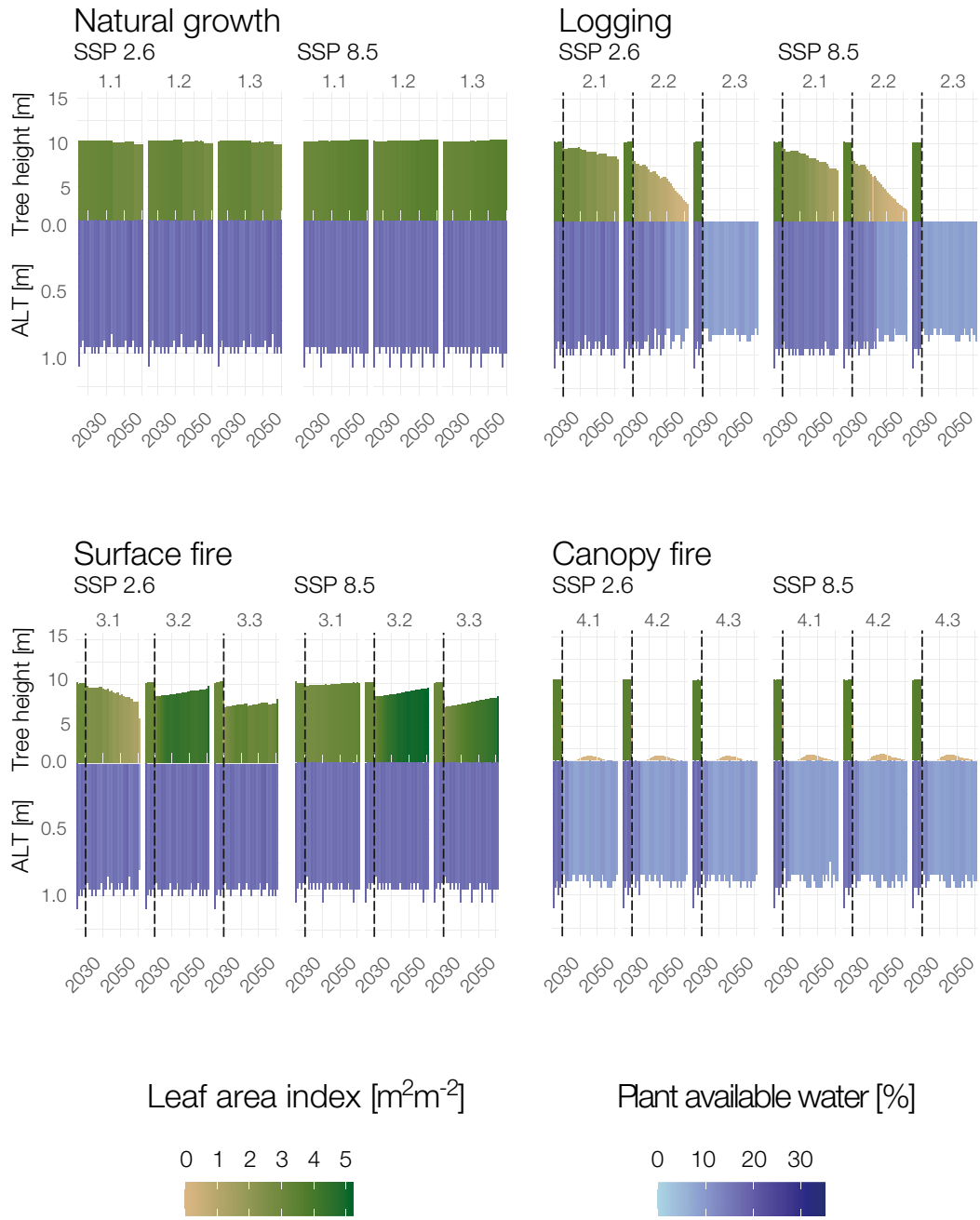

Figure 4. Active layer thickness, tree height, leaf area index and plant available water trajectories for the natural growth scenario, and the logging, and fire (surface and canopy) disturbances under the two climate forcing scenarios SSP2.6 and SSP8.5. Shown is the period from 2015 to 2050 with the disturbance occurring in 2021 (dotted red line) followed by 29 years of recovery.

3.2. Climatic Changes

The average annual air temperature projected for 2020–2050 at our study site is −7.4° C under the SSP1-2.6 scenario and −6.4° C under SSP5-8.5. Under SSP5-8.5 a maximum annual average air temperature of −4.5° C is projected for 2050 (see Figure 3), +2.9° C above the 2021 annual average. Under SSP1-2.6 the change from 2021 to 2050 is +1.0° C. The average total yearly liquid precipitation is 487 mm under SSP1-2.6 and 401 mm under SSP5-8.5. The average total yearly solid precipitation is 196 mm under SSP1-2.6 and 186 mm under SSP5-

8.5 respectively. The average total yearly precipitation (both liquid and solid) is therefore 96 mm higher under SSP1-2.6.

3.3. Forest Stand Development

In the natural growth scenario, where the climate is the only varying factor with yearly average temperatures rising between 1.0 and 2.9° C, our simulations show a very stable development of both active layer thickness (ALT) and plant available water (PAW, volumetric water content [%]). The system stays in an equilibrium state under both climate scenarios, SSP1-2.6 and 5–8.5, for the 29 years analyzed (see Figure 4). While liquid and solid precipitation do not follow a clear trend until 2050, tree density and tree height balance out the temperature changes leaving the ALT and PAW at a constant level throughout the 29 year period. The average ALT under the natural growth scenario shows the lowest variation and is 0.96 m (with a standard deviation (sd) of ±0.1) under SSP1-2.6, and 0.99 m (sd: ± 0.1) under SSP5-8.5 force, respectively. PAW has a mean value of 17.24% (±1.3) under SSP1-2.6%, and 17.03% (±1) under SSP5-8.5, also resulting in the lowest variations compared to the other scenarios. Our simulations further show a decadal height decrease of −0.4 and LAI decrease of −1.2 m^2m^{-2} under SSP1-2.6 climate forcing and a decadal height increase of +2 m and LAI increase of +1.4 m^2m^{-2} under SSP5-8.5. Larch stand density stays constant throughout the entire 29-year period analyzed. In most disturbance scenarios inducing forest loss, the larch forest cover can not reestablish to pre-disturbance states, which will be explained in detail in the following paragraphs on soil moisture and temperature changes. Under SSP5-8.5 forcing we see a faster larch LAI and height decrease for the logging scenario. In the majority of intensity classes of the surface fire scenario we see an increase in forest LAI and tree heights compared to the pre-disturbance state. The surface fire disturbance results in an increasing tree height and LAI for two intensity classes under SSP1-2.6 and all three intensities under SSP5-8.5. This suggests that the surface fire scenario has a positive effect on larch growth within the forest patch.

We find that a decline in larch LAI and tree height is not the case in a majority of intensities of the surface fire scenario. Here, the slight decrease in LAI and average stand height is not followed by an immediate reduction in plant available water. The larch LAI is slowly able to recover in five out of six intensities of the surface fire scenario. Our simulations until 2050 reveal decadal LAI increases up to +3.8 m^2m^{-2} (SSP1-2.6) and +9.5 m^2m^{-2} (SSP5-8.5) and height increases up to +0.9 m (SSP1-2.6) and +1.5 m (SSP5-8.5). The lowest intensity surface fire implemented leads to contrasting forest cover trajectories between the two climate scenarios. In scenario 3.1, the lowest intensity surface fire scenario, LAI shows a decadal trend of −4.8 m^2m^{-2} under SSP1-2.6 but +1.9 m^2m^{-2} under SSP5-8.5 forcing. The tree height decadal trends are −1.8 m (SSP1-2.6) and +0.4 m (SSP5-8.5).

3.4. Post-Disturbance Hydrological Regime of the Ground

We find that a change in larch forest cover has a consistently large impact on the hydrological regime of permafrost at our study site. Under the SSP1-2.6 climate scenario, the average PAW after every disturbance is lower than before with decreases from −2 to −7% (volumetric water content [%]). The largest decrease of −7% is simulated for the canopy fire scenarios where our simulations show complete forest loss just 1 year post-disturbance. The loss in PAW occurs within the first year after the complete forest cover loss. For the natural growth scenario PAW values of up to 20% are simulated. Under SSP5-8.5 forcing post-disturbance PAW is also lower, with decreases from −1 to −7%. The largest decrease is simulated for scenario 4 where the pre-disturbance PAW of 16% (±3) decreases to 9% (±1).

As mentioned above for the lowest intensity surface fire scenario (3.1) our results show contrasting forest cover trajectories between the two climate scenarios SSP1-2.6 and SSP5-8.5. Studying these scenarios plant available water (PAW) values exchanged between our models, we see a high sensitivity of LAI toward small decreases in PAW (see Figure 4 and Figure 5). In scenario 3.1, PAW values under the SSP1-2.6 scenario are lower than under SSP5-5.8 for a number of years starting in the year 2021, 1 year after the disturbance. At this point in time, the LAI trajectories separate and larch forest can not recover in the 3.1 scenario under SSP1-2.6 forcing (see Figure B1).

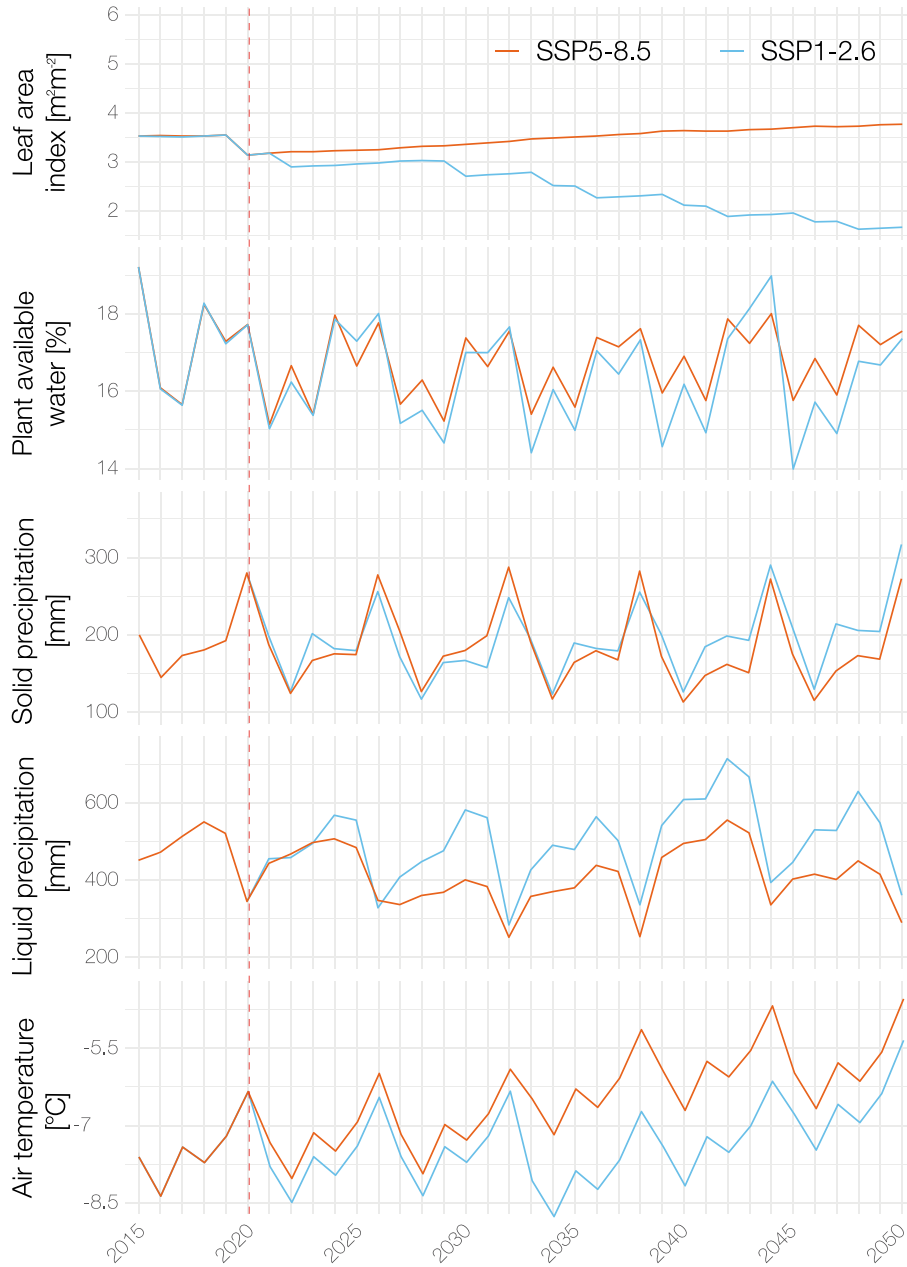

Figure 5. Leaf area index and plant available water trajectories and the forcing for the surface fire scenario 3.1 under the two climate scenarios SSP1-2.6 and SSP5-8.5. Shown is the period from 2015 to 2050 with the disturbance occurring in 2020 followed by 29 years of recovery.

The differences in precipitation and air temperature are small for the studied period until 2050 (see Figure 5). The annual sum of solid and liquid precipitation as well as the annual average air temperature for 2021 (where the LAI trajectories divide) are extremely similar. The sum of the annual precipitation under SSP1-2.6 is 20 mm higher than under SSP5-8.5. Similarly, the annual air temperature is 0.5° C colder under SSP5-8.5 (see Figure 5). We therefore studied the weekly 2021 solid and liquid precipitation patterns in more detail to understand where these small differences in PAW arise, and how they eventually lead to the divergence in LAI. Figure 6 does reveal different precipitation patterns throughout the year between the two climate scenarios. These differences can further be seen in the PAW development throughout the year 2021 and 2022 (see Figure B2). The curves are very similar and only diverge in May, July, August, and September 2021. While SSP1-2.6 shows higher solid

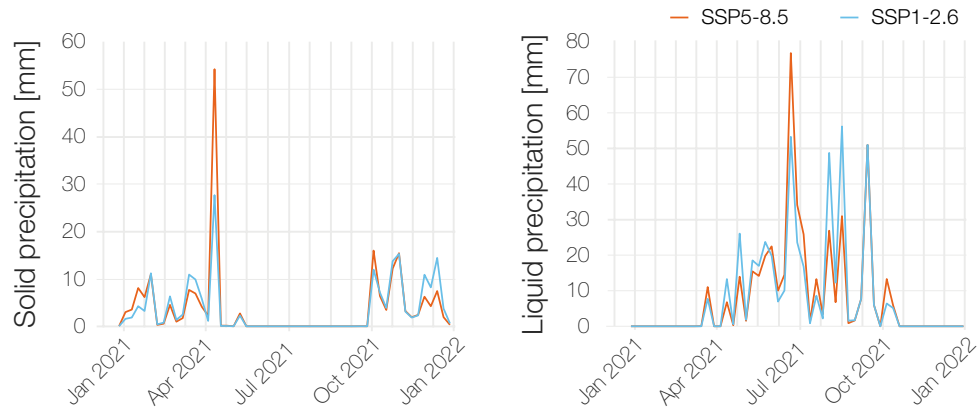

Figure 6. Leaf area index and plant available water trajectories and the forcing for the surface fire scenario 3.1 under the two climate scenarios SSP1-2.6 and SSP5-8.5. Shown is the weekly 2021 solid (left) and liquid (right) precipitation pattern for both climate forcing scenarios.

precipitation values in December and January, the SSP5-8.5 scenario shows high values of solid precipitation in late April. Similarly, under SSP5-8.5 we see an above-average liquid precipitation phase mid-June, while higher liquid precipitation values occur under SSP1-2.6 in fall and early spring. So because the sum of liquid and solid precipitation shows little difference between the two climate forcings, the timing of the precipitation seems to have an effect on the larch forest development. As such, spring and summer precipitation seems to be important for larch forest recovery after disturbance.

3.5. Post-Disturbance Thermal Regime of the Ground

Under SSP1-2.6 the average ALT after disturbance is lower than before with decreases up to −0.1 m in all scenarios. This equals an ALT decrease of −2 to −4%. The largest decrease is simulated for the canopy fire scenario 4.3. Under SSP5-8.5 forcing the average post-disturbance ALT is higher for scenario 3 (+0.1 m) and lower for all other scenarios, with decreases up to −0.1 m. At this very dry site, the latent heat content related to ground ice is small and therefore we do not see large varieties in the ALT over the studied period. The increases in larch LAI following the surface fire scenario have no large impact on the ALT. The simulated differences between SSP1-2.6 and 5–8.5 are surprisingly small with ALT differences below 0.1 m.

4. Discussion

4.1. Larch Forest Recovery and Disturbances Under a Warming Climate

The natural growth simulations show that larch height and LAI play an important role in controlling the permafrost conditions underneath and maintaining the ecosystem's stable conditions. Under natural growth, our model simulates a stable development for both climate scenarios until 2050. At SPA this stable trajectory was also found in a previous study by Sato et al. (2016), while larch forest is declining in some southern, drought-prone regions and expanding at the northern treeline (i.e., Mamet et al. [2019]). In central Yakutia, this trend is not visible for the studied period until 2050. Our simulations reveal decadal tree height increases between +0.9 m (SSP1-2.6) and +1.5 m (SSP5-8.5) which is in line with a previous assessment of the potential tree height increases in Siberia. Tchebakova et al. (2016) reported height increases until 2080 in light deciduous larch forests between 5 and 15 m depending on the climate projection.

Our simulations show that the plant available water (PAW) and the thawing conditions control the recovery of larch. The disturbance scenarios all lead to a change in LAI, tree height, ALT and PAW at varying degrees. Logging and canopy fire scenarios, with high mortality rates, lead to a consistent loss of larch forest cover and very low PAW values. Generally, lower LAI leads to decreasing transpiration through the vegetation which can lead to wetting of the ground (O'Donnell et al., 2011) but sandy soils offer good drainage conditions which

enhance the drying of the ground at this study site (see also i.e., Zhang et al. [2011]). In previous studies we have additionally found higher snowpacks in dense forests, hence there is higher availability of melt water in spring (Stuenzi, Boike, Cable, et al., 2021). The substantial decrease in soil moisture presented here cannot sustain constant larch conditions (LAI and height) nor trigger the reestablishment of pre-disturbance larch tree heights and LAIs within the studied 29 years. A decline in LAI and tree height is consistent for all intensities of the logging and canopy fire scenarios. This is in agreement with the study conducted by Takahashi (2006) at Spasskaya pad where they found a post-fire reforestation period of 30–35 years with a likely change in dominant species from the light conifer larch or dark conifers such as spruce, fir or cedar, to soft deciduous (birch or aspen), to mixed forests. The modeling setup here does not simulate the growth of different taxa. Several studies have found that burned forest patches can serve as ecological niches for evergreen needleleafs and deciduous broadleafs (V. I. Kharuk et al., 2005; V. Kharuk et al., 2007; Y. Liu et al., 2017). Furthermore, moderate burn severity has shown a high rate of larch recruitment while high-severity burns favor the growth of shrubs, grasses, and broadleaf trees and possibly never recover to the previous dominance of larch (Chu et al., 2017). Our results suggest that larch forests generally thrive after surface fires which could be an important factor for larch forest persistence. This is in agreement with previous studies claiming that larch are less vulnerable to surface fires than other conifers and the ecosystem is most accustomed to this type of disruption because it is the most common disturbance (Ponomarev et al., 2016; Schulze et al., 2012; Takahashi, 2006). Accordingly, surface fire is a regular phenomenon that is important for the stability, productivity, and carbon sequestration in the fire-adapted coniferous forests of Siberia (Alexander et al., 2012; Wirth, 2005). Our simulations even show increased larch LAIs and heights after surface fires.

Our simulations of the surface fire scenario finally reveal that small differences in precipitation can potentially change the trajectory of the tightly coupled forest-permafrost ecosystem. Notably, small differences in weather patterns, such as the differences in the timing of precipitation events found here, or extreme weather events can also be dampened in a natural forest, that is, because of bushy undergrowth which impacts snow depth, snow redistribution, lateral surface water flow, shading, etc.

Furthermore, it is clearly visible that the LAI decreases every time PAW values reach the critical threshold of 15%. In on intensity (3.1), this threshold is reached, while for the other two intensities of the surface fire scenario, PAW values are very similar under both climate scenarios and LAI can recover or even surpass pre-disturbance conditions because the critical value of 15% is not reached (see Figure B1). Wherever the threshold of 15% is reached, such as in the 3.3 subarea, in the years 2032 and 2044, we also see the effect of the 10% growth penalty with its related LAI decrease. We recognize that this is a set parameter within our model setup which is highly important for the forest trajectory. This value is derived from the literature value of the lower boundaries of the optimum water availability which is 21.1% for larch as defined by (Sato et al., 2010). The set threshold of 15% as the critical PAW value as well as the 10% growth penalty introduced thereafter is highly relevant in terms of the larch forest trajectories simulated here. To understand where exactly these thresholds lay, the two values need to be further evaluated in field studies to improve the validity of the model threshold and to make even better projections for larch forest development after disturbances.

Wherever the exact threshold value occurs in nature, drought-like states which lead to the under-passing of this plant's available water value can trigger larch forest decline. In our simulations, larch cover loss increases the chance that the PAW value falls below the 15% threshold again. This finding is an indicator for a feedback behavior between plant available water and larch growth and is in line with previous findings. Zhang et al. (2011) found that the trees maintain permafrost through radiation interception and control the freeze-thaw dynamics in summer. The limited ALT in summer then guarantees sufficient moisture availability for trees and further lowers the frequency of fires. Zhang et al. (2011) furthermore found that this tightly coupled system cannot be maintained beyond a warming of about +2° C. Previous studies using the model framework applied here have found that the forest has a net stabilizing effect on the permafrost ground at Spasskaya pad. The main controlling mechanism behind this is canopy shading, along with enhanced longwave radiation (due to low below-canopy windspeeds resulting in low turbulent fluxes), higher groundwater content, and a higher snowpack. Forest loss was found to lead to higher ground surface temperatures in the snow-free and the snow-covered periods, and a doubling of the plant available water in the thawed active layer in the summer, resulting in an active layer thickness increase of 25% (Stuenzi, Boike, Cable, et al., 2021; Stuenzi, Boike, Gädeke, et al., 2021).

The introduced shift in ground surface albedo after the fire scenarios and the inability of the model to simulate a vegetation cover with an LAI below 0.7 m^2m^{-2} introduce some uncertainty in our modeling results. Accordingly, we have compared the results of the highest intensity canopy fire scenario which includes larch forest loss, a changed ground surface albedo, and the removal of the organic layer (scenario 4.3, see Figure 2) to the logging scenarios where these parameters were not modified (see scenario 2.3, which includes the complete removal of larch trees but no modification to the albedo or the organic layer). As such, under the SSP5-8.5 scenario, the average PAW in the first 5 years after the disturbance in the high-intensity logging scenario is 8.7% (SD: 0.6) and the same value is 11.3% (SD: 1.6) in the canopy fire scenario. The average maximum ALT of the first 5 years after the disturbance is 0.9 m (SD: 0.03) in the logging scenario and 0.9 m (SD: 0.04) in the canopy fire scenario. Under the SSP1-2.6 scenario, the 5 years post-disturbance average PAW in the logging scenario is 8.9% (SD: 0.7) and 11.4 m (SD: 1.5) in the surface fire scenario. Here, the average maximum ALT of the first 5 years after the disturbance is 0.8 m (SD: 0.05) in the logging scenario and 0.9 m (SD: 0.04) in the canopy fire scenario. The differences between the two scenarios with complete larch forest removal in 2020 are a result of the combined effects of the litter and organic layer damage and the ground surface albedo change. The differences in PAW between the two scenarios are 2.6% (SSP5-8.5) and 2.5% (SSP1-2.6), which is much smaller than the differences found between the pre- and post-disturbance states. Following the comparison of these two scenarios, we are confident that the change in PAW is largely due to the loss of larch forest and not a result of the ground surface albedo or organic layer change.

Regeneration in the North is slow due to small turnover rates and short growing seasons. Stand-replacing disturbances were found to cause succession with a change in dominant species (Takahashi, 2006). A typical progression for larch-dominated ecosystems progresses from deciduous needleleaf towards deciduous broadleaf (mostly birch or aspen) to mixed deciduous and evergreen needleleaf (mostly spruce or pine). In our simulations, we do not account for these successional stages or the growth of taxa besides larch. Succession towards a deciduous broadleaf or evergreen needleleaf-dominated forest would nevertheless also modify the surface energy balance of the ground (Stuenzi, Boike, Gädeke, et al., 2021; Zhang et al., 2011). The resulting changes to the surface energy balance and hence the ground thermal and hydrological regime could potentially again lead to conditions suitable for larch reestablishment, assuming the availability of nearby seed sources. Our model further does not include size-based mortality impacts of fires or the effects of reoccurring disturbances. Especially the establishment of evergreen taxa highly depends on the frequency of disturbance events, which has increased over the past few decades (Mekonnen et al., 2019; Meredith et al., 2019; Shuman et al., 2011). Furthermore, larger disturbed areas are likely to favor the establishment of deciduous broadleaf (mostly birch) as they have a wider seed dispersal range and higher reproduction capability than evergreen or deciduous needleleaf which are much more limited by seed dispersal (Otoda et al., 2013; Rogers et al., 2015). Accordingly, Z. Liu (2016) found that post-fire recovery mainly depends on seed availability in relation to fire severity and spatial extent. Additionally, the germination and successful establishment of saplings are controlled by moisture conditions and local site characteristics. In our simulations, seed availability does not seem to be a deciding factor for the successful establishment of larch trees after disturbance. Following the model spin-up period where after the simulated larch forest stands are in equilibrium with climate, the difference in LAI is insignificant between 0, 100, and 200 seeds/year/hectare (see Figure C1). Therefore, the establishment is mostly determined by the local site and moisture conditions. The tree removal simulated in the disturbance scenarios as well as the missing competition by early-successor species (mostly deciduous broadleaf (Takahashi, 2006)) allows for increased resource access for larch saplings. This might lead to an overestimation of larch regrowth. Finally, in our modeling setup the organic layer thickness is based on observations and does not change in composition or quality based on the upper storey vegetation. The thickness and content of the organic layer do have a large impact on the surface energy balance of the ground and should therefore be further explored (see e.g., Foster et al. [2019]). In this case study, we try to understand the rather short-term impacts of typical disturbance scenarios. The focus lies on the differences between a variety of common scenarios. We do not assess the frequency or the effect of multiple overlapping disturbances which would be an important process to look at in further studies. We focus on the most common disturbances while there are many more scenarios to be studied, among others droughts, windfalls, or pests, which have also been reported to increase in number or intensity under climatic changes (V. I. Kharuk et al., 2021).

In summary, our simulations show that whether larch forests can return to a larch-dominated post-disturbance state is also dependent on permafrost dynamics, mainly the hydrological conditions of the ground. Within our

modeling framework, we find indicators that dry or wet years following the disturbances as well as the timing of the precipitation throughout the seasons, can affect the larch reestablishment.

5. Conclusions

We find that ecosystem resilience toward different disturbances depends on the intensity and the type of disturbance event. We used a coupled larch dynamics permafrost model and applied different disturbance scenarios, such as surface and canopy fires and logging. Our modeling study is in agreement with observations that have shown that larch forests foster resilience against regional, typical fire regimes, such as the surface fire scenario implemented here. In contrast, the larch forest simulated here remains severely disturbed after the other disturbances (canopy fire and logging) studied here. We find that after such disturbances the ground becomes drier and the larch forests do not recover to pre-disturbance larch densities within the 29 years analyzed. We further find that the amount of precipitation, as well as the timing of precipitation events within the individual years after disturbances, can affect the larch forest trajectory. This points to a threshold-bound tipping behavior of larch forests to changes in plant-available soil moisture. Further studies on exact threshold values for plant-available soil water and related growth penalties for larch taxa are needed.

The main findings of our study can be summarized as follows:

1. We find that disturbances with high mortality rates, such as canopy fires and logging, lead to a reduction in plant-available soil water by up to −44%. This results in a continuous decline of larch forest cover
2. Only surface fires, the most common disturbance type, can lead to an increased larch density and constant soil moisture values over the studied period of 29 years
3. Finally, we find that the trajectory of larch forests after surface fires is dependent on the precipitation conditions in the years after the disturbance. Dryer years can change the direction of the larch forest development within the studied period

Here, we demonstrate the capabilities of a dynamic multilayer-forest-permafrost model in simulating the complex interactions and feedbacks between boreal forest cover, permafrost, climate, and disturbances. Our study provides an overview of possible mid-term permafrost and larch forest trajectories after different disturbance scenarios that disrupt the tightly coupled ecosystem. These findings are particular to dry, larch-dominated, and permafrost-underlain larch forests in eastern Siberia. Nevertheless, our study has implications for other boreal areas because our model showcases how fragile the quasi-equilibrium between active layer thickness, plant-available soil moisture, disturbances, and forest cover is.

Appendix A: Model Parameters Used and Constants

Table A1
Overview of the CryoGrid Parameters Used

Process/Parameter		Value	Unit	Source
Density falling snow	ρ_{snow}	80–200	kg m^{-3}	Stuenzi, Boike, Gädeke et al. (2021)
Ground surface albedo	α	0.15	-	*field measurement*
Roughness length	z_0	0.001	m	Westermann et al. (2016)
Roughness length snow	z_{0snow}	0.0001	m	Boike et al. (2019)
Geothermal heat flux	F_{lb}	0.05	W m^{-2}	Westermann et al. (2016)
Thermal cond. mineral soil	$k_{mineral}$	3.0	W m^{-1} K^{-1}	Westermann et al. (2016)
Emissivity	ϵ	0.99	-	Langer et al. (2011)
Root depth	D_T	0.2	m	*field measurement*
Evaporation depth	D_E	0.1	m	Nitzbon et al. (2019)
Hydraulic conductivity	K	10^{-5}	m s^{-1}	Boike et al. (2019)

Table A2
Overview of the LAVESI Parameters Used

Parameter	*Larix gmelinii*	Reference
Minimum active layer	20	Abaimov et al. (1998)
January threshold temperature	−45C	Kruse et al. (2016, 2018, 2019)
Minimum soil water	21.1% vol.	Sato et al. (2010)
Mortality drought	0.237805	Kruse et al. (2016, 2018, 2019)
Rooting depth	50	Abaimov et al. (1998)
Maximum age	609	Kruse et al. (2016, 2018, 2019)
Mortality age	8.18785	Kruse et al. (2016, 2018, 2019)
Resprouting	0.01	Kruse et al. (2016, 2018, 2019)

Table A3
Parameter Set-Up for the Study Site

Study site	Tree height(m)	Soil layer depth(Litter/Organic/Mineral)	Respective soil type	ERA-interim coordinate
Spasskaya	12	0/0.08/0.16	Peat/Clay/Sand	N 62.14, E 129.37

Table A4
Constants

Constants	Value	Unit
von Karman	0.4	-
Freezing point water (normal pres.)	273.15	K
Latent heat of vapourization	2.501 × 10^6	J kg^{-1}
Molecular mass of water	18.016	g mol^{-1}
Molecular mass of dry air	28.966	g mol^{-1}
Specific heat dry air (const. pres.)	1004.64	J kg^{-1} K^{-1}
Density of fresh water	1000	kg m^{-3}
Heat of fusion for water at 0° C	0.334 × 10^6	J kg^{-1}
Thermal conductivity of water	0.57	W m^{-1} K^{-1}
Thermal conductivity of ice	2.2	W m^{-1} K^{-1}
Kinem. visc. air (0° C, 1013.25 hPa)	0.0000133	m^2 s^{-1}
Sp. heat water vapor (const. pr.)	1810	J kg^{-1} K^{-1}

Table A5
Multilayer Canopy Parameters for Deciduous Needleleaf (NDT) Plant Functional Type

Parameter	Value	Unit	Source
Leaf angle dep. from spherical	0.01	-	Bonan (2002)
Leaf reflectance (VIS/NIR)	0.07/0.35	-	Bonan (2002)
Stem reflectance (VIS/NIR)	0.16/0.39	-	Bonan (2002)
Leaf transmittance (VIS/NIR)	0.05/0.01	-	Bonan (2002)
Stem transmittance (VIS/NIR)	0.001/0.001	-	Bonan (2002)
Max. carboxylation rate (25° C)	43	μmol m^{-2} s^{-1}	Bonan (2002)
Photosynthetic pathway	C3	-	Bonan (2002)
Leaf emissivity	0.98	-	Bonan (2002)
Leaf dimension	0.04	m	Bonan (2002)
Roughness length	0.055	m	Bonan (2002)
Displacement height	0.67	m	Bonan (2002)
Root distribution (a/b)	7.0/2.0	-	Bonan (2002)
Min. vapor pressure deficit	100	Pa	Bonan (2019)
Plant capacitance	2500	mmol H_2O m^{-2} leaf area MPa^{-1}	Bonan (2019)
Minimum leaf water potential	−2	MPa	Bonan (2019)
Stem hydraulic conductance	4	mmol H_2O m^{-2} s^{-1} leaf area MPa^{-1}	Bonan (2019)
Atmospheric CO_2	380	μmol mol^{-1}	Bonan (2019)
Atmospheric O_2	209	mmol mol^{-1}	Bonan (2019)
Soil evaporative resistance	3361.509	s m^{-1}	Bonan (2019)
Specific heat of dry-wet soil	1396	J kg^{-1} K^{-1}	Oleson et al. (2013)
Specific heat of fresh H_2O	4188	J kg^{-1} K^{-1}	Oleson et al. (2013)
Specific leaf area (TOC)	0.024	m^2 g^{-1} C	Bonan et al. (2018)
Fine root biomass	500	g biomass m^{-2}	Bonan (2019)
Leaf drag coefficient	0.25	-	Bonan (2019)
Foliage clumping index	0.7	-	Bonan (2019)

Appendix B: Plant Available Water Trajectories After Surface Fire

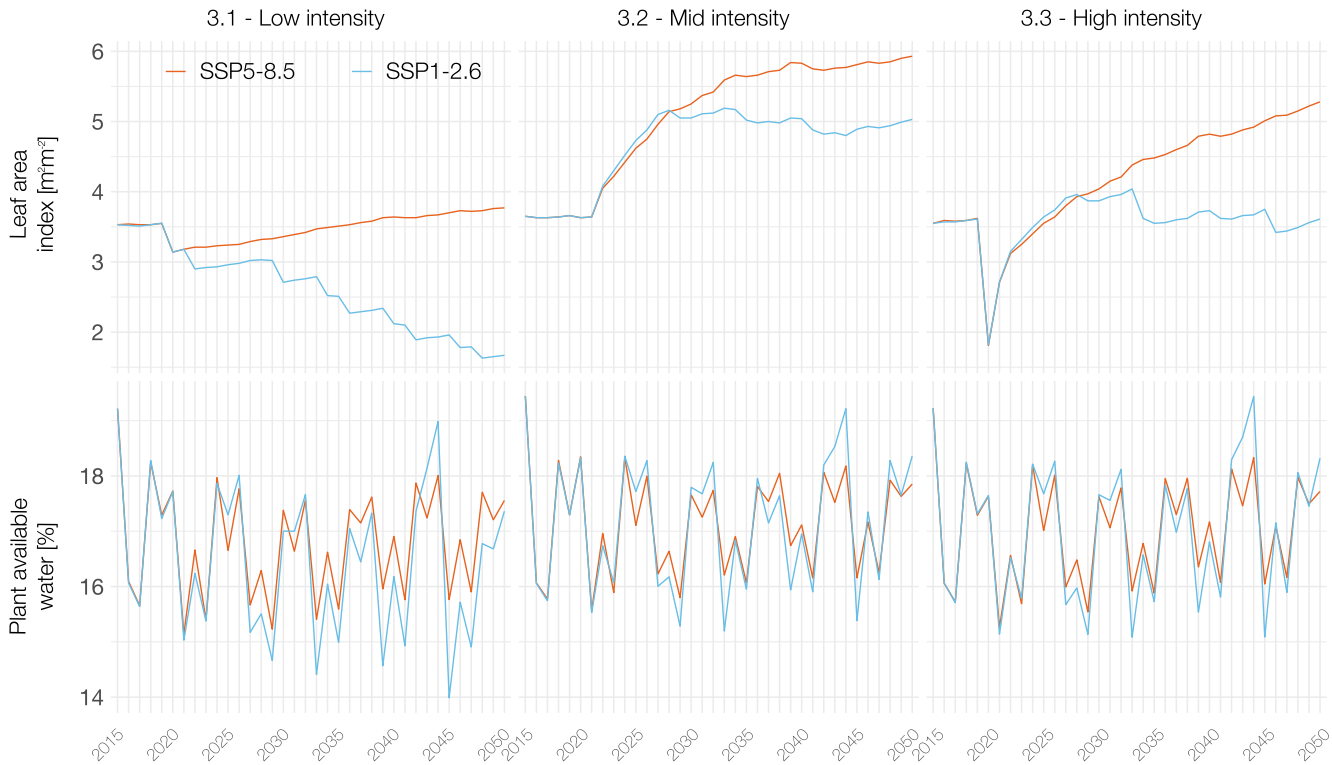

Figure B1. Leaf area index and plant available water trajectories for the surface fire scenarios 3.1–3.3 under the two climate scenarios SSP1-2.6 and SSP5-8.5. Shown is the period from 2015 to 2050 with the disturbance occurring in 2020 followed by 29 years of recovery.

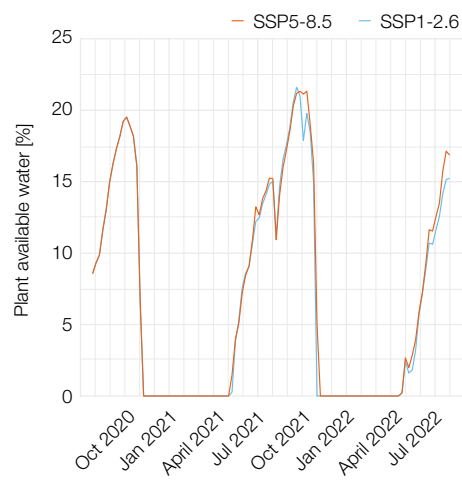

Figure B2. Weekly plant available water trajectories for the surface fire scenario 3.1 under the two climate scenarios SSP1-2.6 and SSP5-8.5. Shown is the period from July 2020-August 2022.

Appendix C: Model Verification

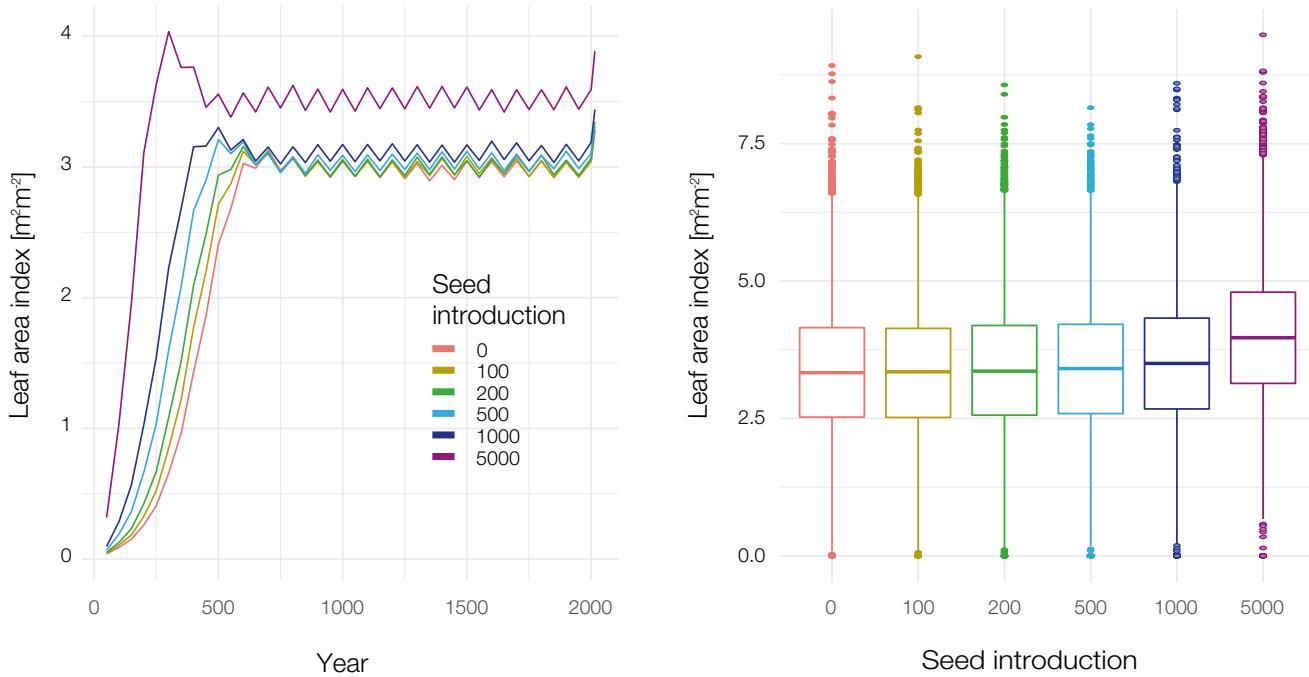

Figure C1. Simulation experiment at our study site using LAVESI with different levels of permanent seed introduction. Left: At the beginning of the LAVESI simulation (exponential phase) the introduction of seeds and the average LAI value show a positive effect and more introduced seeds lead to a quicker population growth. However, the differences between 0 and 500 seeds become insignificant after 700 simulation years. Right: The LAI values across the entire simulation area do not differ between the introduction of 100, 200, 500, or even 1,000 seeds/yr/ha. The mean LAI values are 3.28 ± 1.34 with 0 seeds, 3.28 ± 1.33 with 100, 3.31 ± 1.33 with 200, 3.34 ± 1.34 with 500, 3.44 ± 1.36 with 1,000, and 3.89 ± 1.44 with 5,000, respectively. The difference in means is insignificant between 0 and 100 (Welch-two sample *t*-test, $p = 0.821$) and 0 and 200 ($p = 0.061$), but significantly different beginning with 500 seeds ($p < 0.001$).

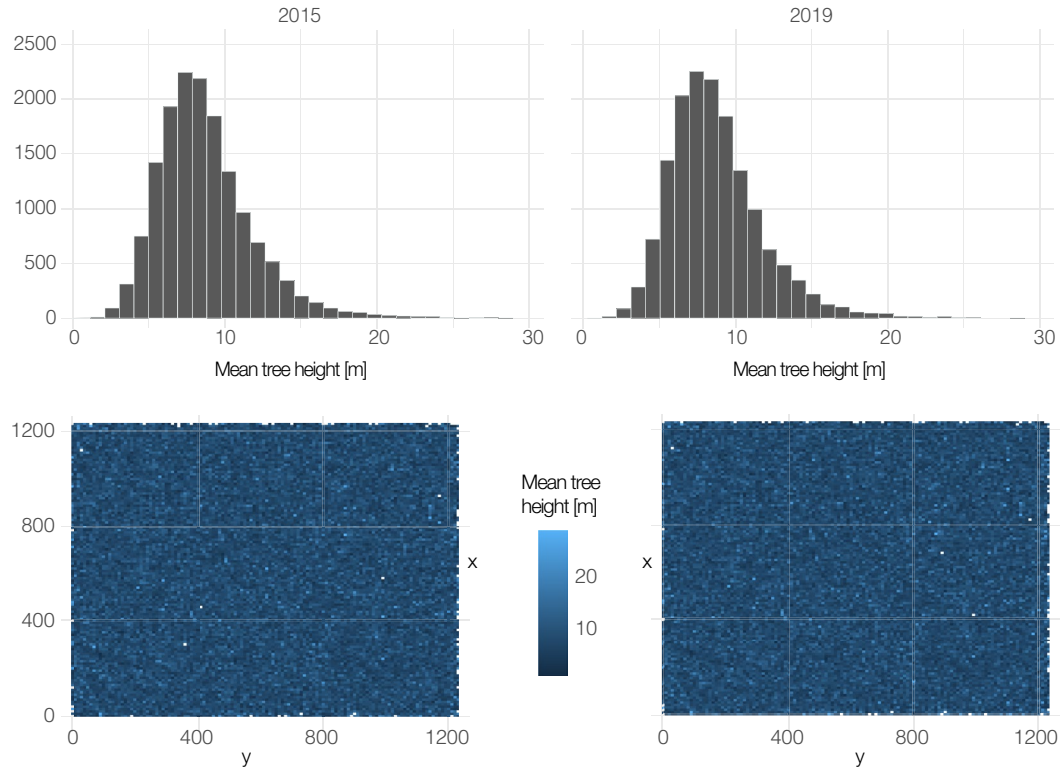

Figure C2. Top: Histogram of simulated mean LAVESI tree heights [m] for 2015 (before coupling) and 2019 (after coupling). Bottom: Tree height distribution in the LAVESI simulated forest plot for 2015 and 2019.

Conflict of Interest

The authors declare no conflicts of interest relevant to this study.

Data Availability Statement

The CryoGrid-Vegetation code developed for the use with LAVESI is available on Zenodo https://doi.org/10.5281/zenodo.5119987 (Stuenzi, Kruse, et al., 2021). Accordingly, the LAVESI code for the coupled model version used here is available on Github https://github.com/StefanKruse/LAVESI/releases/tag/1.0 and permanently stored on Zenodo https://doi.org/10.5281/zenodo.5963455 (Kruse, Stuenzi, & Gloy, 2022). Hersbach, H. et al. (2018) was downloaded from the Copernicus Climate Change Service (C3S) Climate Data Store. The results contain modified Copernicus Climate Change Service information 2020. Neither the European Commission nor ECMWF is responsible for any use that may be made of the Copernicus information or data it contains. This supporting information section contains model parameters and constants for CryoGrid-Vegetation and Lavesi, as well as the parameter set-up for the study site.

References

Abaimov, A. P., Lesinski, J. A., Martinsson, O., & Milyutin, L. I. (1998). *Variability and ecology of Siberian larch species (Tech. Rep.)*. Swedish University of Agricultural Sciences, (SLU), Department of Silviculture. Retrieved from https://www.osti.gov/etdeweb/servlets/purl/10147794

Alexander, H. D., Mack, M. C., Goetz, S., Loranty, M. M., Beck, P. S. A., Earl, K., et al. (2012). Carbon accumulation patterns during post-fire succession in Cajander larch (Larix cajanderi) forests of Siberia. *Ecosystems*, *15*(7), 1065–1082. https://doi.org/10.1007/s10021-012-9567-6

AsiaFlux. (2017). *Yakutsk Spasskaya pad larch forest data (site code: YLF)*. Retrieved from http://asiaflux.net/index.php?page_id=121

Averensky, A., Chikidov, I. I., & Ermakova, Y. V. (2010). Insect impact on vegetation. In E. I.Troeva (Ed.), *The far north: Plant biodiversity and ecology of yakutia, plant and vegetation* (3rd ed., pp. 297–316). Springer. https://doi.org/10.1007/978-90-481-3774-9_5

Baldocchi, D. D., Xu, L., & Kiang, N. (2004). How plant functional-type, weather, seasonal drought, and soil physical properties alter water and energy fluxes of an oak–grass savanna and an annual grassland. *Agricultural and Forest Meteorology*, *123*(123), 13–39. Retrieved from https://doi.org/10.1016/j.agrformet.2003.11.006

Acknowledgments
SMS is thankful to the POLMAR graduate school, the Geo.X Young Academy and the WiNS program at the Humboldt Universität zu Berlin for providing a supportive framework for her research. SMS is very grateful for the help during fieldwork in 2018 and 2019, especially for the help from Levina Sardana Nikolaevna, Alexey Nikolajewitsch Pestryakov, Lena Ushnizkaya, Luise Schulte, Frederic Brieger, Stuart Vyse, Elisbeth Dietze, Nadine Bernhard, Boris K. Biskaborn, Iuliia Shevtsova, as well as Luidmila Pestryakova and Evgeniy Zakharov. Additionally, SMS would like to thank Stephan Jacobi, Alexander Oehme, Niko Borneman, Peter Schreiber and William Cable for their help in preparing for field work and the entire PermaRisk and Sparc research groups for their ongoing support. Finally, SMS would like to thank the editor and anonymous reviewers for their comments and suggestions which have greatly improved the paper. This study has been supported by the ERC consolidator grant Glacial Legacy to Ulrike Herzschuh (no. 772852). Further, the work was supported by the Federal Ministry of Education and Research (BMBF) of Germany through a grant to Moritz Langer (no. 01LN1709 A). Funding was additionally provided by the Helmholtz Association in the framework of MOSES (Modular Observation Solutions for Earth Systems). Sebastian Westermann acknowledges funding by Permafost4Life (Research Council of Norway, grant no. 301639) and ESA Permafrost_CCI (climate.esa.int/en/projects/permafrost/). Open access funding enabled and organized by Projekt DEAL.

Baltzer, J. L., Veness, T., Chasmer, L. E., Sniderhan, A. E., & Quinton, W. L. (2014). Forests on thawing permafrost: Fragmentation, edge effects, and net forest loss. *Global Change Biology*, *20*, 824–834. https://doi.org/10.1111/gcb.12349

Boike, J., Nitzbon, J., Anders, K., Grigoriev, M., Bolshiyanov, D., Langer, M., et al. (2019). A 16-year record (2002-2017) of permafrost, active-layer, and meteorological conditions at the Samoylov Island arctic permafrost research site, Lena river delta, northern Siberia: An opportunity to validate remote-sensing data and land surface, snow, and. *Earth System Science Data*, *11*, 261–299. https://doi.org/10.5194/essd-11-261-2019

Bonan, G. B. (2002). *Ecological climatology: Concepts and applications*: Cambridge University Press.

Bonan, G. B. (2019). *Climate change and terrestrial ecosystem modeling*. Cambridge University Press. https://doi.org/10.1017/9781107339217

Bonan, G. B., Patton, E. G., Harman, I. N., Oleson, K. W., Finnigan, J. J., Lu, Y., & Burakowski, E. A. (2018). Modeling canopy-induced turbulence in the Earth system: A unified parameterization of turbulent exchange within plant canopies and the roughness sublayer (CLM-ml v0). *Geoscientific Model Development*, *11*(4), 1467–1496. https://doi.org/10.5194/gmd-11-1467-2018

Bonan, G. B., Pollard, D., & Thompson, S. L. (1992). Effects of boreal forest vegetation on global climate. *Nature*, *359*(6397), 716–718. https://doi.org/10.1038/359716a0

Bonan, G. B., & Shugart, H. H. (1989). In *Environmental Factors and Ecological Processes in Boreal Forests* (Vol. 20, Tech. Rep.). https://doi.org/10.1146/annurev.es.20.110189.000245

Bonan, G. B., Williams, M., Fisher, R. A., & Oleson, K. W. (2014). Modeling stomatal conductance in the Earth system: Linking leaf water-use efficiency and water transport along the soil-plant-atmosphere continuum. *Geoscientific Model Development*, *7*(5), 2193–2222. https://doi.org/10.5194/gmd-7-2193-2014

Carpino, O. A., Berg, A. A., Quinton, W. L., & Adams, J. R. (2018). Climate change and permafrost thaw-induced boreal forest loss in northwestern Canada. *Environmental Research Letters*, *13*, 084018. https://doi.org/10.1088/1748-9326/aad74e

Chang, X., Jin, H., Zhang, Y., He, R., Luo, D., Wang, Y., et al. (2015). Thermal impacts of Boreal forest vegetation on active layer and permafrost soils in Northern da Xing'Anling (Hinggan) Mountains, Northeast China. *Arctic Antarctic and Alpine Research*, *47*(2), 267–279. https://doi.org/10.1657/AAAR00C-14-016

Chasmer, L., Quinton, W., Hopkinson, C., Petrone, R., & Whittington, P. (2011). Vegetation canopy and radiation controls on permafrost plateau evolution within the discontinuous permafrost zone, Northwest Territories, Canada. *Permafrost and Periglacial Processes*, *22*(3), 199–213. https://doi.org/10.1002/ppp.724

Chen, D., & Loboda, T. V. (2018). Surface forcing of non-stand-replacing fires in Siberian larch forests. *Environmental Research Letters*, *13*(4), 2002–2011. https://doi.org/10.1088/1748-9326/aab443

Chen, D., Loboda, T. V., He, T., Zhang, Y., & Liang, S. (2018). Strong cooling induced by stand-replacing fires through albedo in Siberian larch forests. *Scientific Reports*, *8*(1), 1–10. https://doi.org/10.1038/s41598-018-23253-1

Chu, T., Guo, X., & Takeda, K. (2017). Effects of burn severity and environmental conditions on post-fire regeneration in Siberian larch forest. *Forests*, *8*(3), 76. https://doi.org/10.3390/f8030076

Fisher, J. P., Estop-Aragonés, C., Thierry, A., Charman, D. J., Wolfe, S. A., Hartley, I. P., et al. (2016). The influence of vegetation and soil characteristics on active-layer thickness of permafrost soils in boreal forest. *Global Change Biology*, *22*(9), 3127–3140. https://doi.org/10.1111/gcb.13248

Foster, A. C., Armstrong, A. H., Shuman, J. K., Shugart, H. H., Rogers, B. M., Mack, M. C., et al. (2019). Importance of tree- and species-level interactions with wildfire, climate, and soils in interior Alaska: Implications for forest change under a warming climate. *Ecological Modelling*, *409*, 108765. https://doi.org/10.1016/J.ECOLMODEL.2019.108765

Giglio, L., Descloitres, J., Justice, C. O., & Kaufman, Y. J. (2003). An enhanced contextual fire detection algorithm for MODIS. *Remote Sensing of Environment*, *87*, 273–282. https://doi.org/10.1016/S0034-4257(03)00184-6

Harman, I. N., Finnigan, J. J., Harman, I. N., & Finnigan, J. J. (2008). Scalar concentration profiles in the canopy and roughness sublayer. *Boundary-Layer Meteorology*, *129*(3), 323–351. https://doi.org/10.1007/S10546-008-9328-4

Harris, I., Osborn, T. J., Jones, P., & Lister, D. (2020). Version 4 of the CRU TS monthly high-resolution gridded multivariate climate dataset. *Scientific Data*, *7*(109). https://doi.org/10.1038/s41597-020-0453-3

Helbig, M., Pappas, C., & Sonnentag, O. (2016). Permafrost thaw and wildfire: Equally important drivers of boreal tree cover changes in the Taiga Plains, Canada. *Geophysical Research Letters*, *43*(4), 1598–1606. https://doi.org/10.1002/2015GL067193

Hersbach, H., Bell, B., Berrisford, P., Biavati, G., Hanányi, A., Munoz Sabater, J., et al. (2018). ERA5 hourly data on single levels from 1979 to present. *Copernicus climate change Service (C3S) climate data Store (CDS)*. https://doi.org/10.24381/cds.adbb2d47

Holloway, J. E., Lewkowicz, A. G., Douglas, T. A., Li, X., Turetsky, M. R., Baltzer, J. L., & Jin, H. (2020). Impact of wildfire on permafrost landscapes: A review of recent advances and future prospects. *Permafrost and Periglacial Processes*, *31*(3), 371–382. https://doi.org/10.1002/ppp.2048

Jin, X. Y., Jin, H. J., Iwahana, G., Marchenko, S. S., Luo, D. L., Li, X. Y., & Liang, S. H. (2020). Impacts of climate-induced permafrost degradation on vegetation: A review. *Advances in Climate Change Research*, *12*(1), 29–47. https://doi.org/10.1016/j.accre.2020.07.002

Jin, Y., Randerson, J. T., Goetz, S. J., Beck, P. S., Loranty, M. M., & Goulden, M. L. (2012). The influence of burn severity on postfire vegetation recovery and albedo change during early succession in North American boreal forests. *Journal of Geophysical Research*, *117*(1), 1036. Retrieved from https://doi.org/10.1029/2011JG001886

Kajimoto, T. (2010). Root system development of larch trees growing on Siberian permafrost. In A.Osawa, O.Zyryanova, Y.Matsuura, T.Kajimoto, & R.Wein (Eds.), *Permafrost ecosystems. Ecological studies (analysis and synthesis)* (Vol. 209, pp. 303–330). Springer. https://doi.org/10.1007/978-1-4020-9693-8_16

Kelliher, E., Schulze, E.-D., Bauer, G., & Arneth, A. (1998). Forest-atmosphere carbon dioxide exchange in eastern Siberia. *Agricultural and Forest Meteorology*, *90*, 291–306. https://doi.org/10.1016/S0168-1923(98)00057-4

Kharuk, V., Ranson, K., & Dvinskaya, M. (2007). Evidence of evergreen conifer invasion into larch dominated forests during recent decades in central Siberia. *Eurasian Journal of Forest Research*, *10*(2), 163–171. Retrieved from https://eprints.lib.hokudai.ac.jp/dspace/bitstream/2115/30308/1/10%282%29_163-171.pdf

Kharuk, V. I., Dvinskaya, M. L., Ranson, K. J., & Im, S. T. (2005). Expansion of evergreen conifers to the larch-dominated zone and climatic trends. *Russian Journal of Ecology*, *36*(3), 164–170. https://doi.org/10.1007/s11184-005-0055-5

Kharuk, V. I., Ponomarev, E. I., Ivanova, G. A., Dvinskaya, M. L., Coogan, S. C., & Flannigan, M. D. (2021). Wildfires in the Siberian taiga. *Ambio*, *50*, 1953–1974. https://doi.org/10.1007/s13280-020-01490-x

Kharuk, V. I., Ranson, K. J., & Dvinskaya, M. L. (2010). Wildfire dynamics in mid-Siberian larch dominated forests. *Advances in Global Change Research*, *40*, 83–100. https://doi.org/10.1007/978-90-481-8641-9_6

Kharuk, V. I., Ranson, K. J., Dvinskaya, M. L., & Im, S. T. (2011). Wildfires in northern Siberian larch dominated communities. *Environmental Research Letters*, *6*(4), 045208. https://doi.org/10.1088/1748-9326/6/4/045208

Kharuk, V. I., Ranson, K. J., Petrov, I. A., Dvinskaya, M. L., Im, S. T., & Golyukov, A. S. (2019). Larch (Larix dahurica Turcz) growth response to climate change in the Siberian permafrost zone. *Regional Environmental Change*, *19*(1), 233–243. https://doi.org/10.1007/s10113-018-1401-z

Kirichenko, N. I., Baranchikov, Y. N., & Vidal, S. (2009). Performance of the potentially invasive Siberian moth *Dendrolimus superans sibiricus* on coniferous species in Europe. *Agricultural and Forest Entomology*, *11*(3), 247–254. https://doi.org/10.1111/j.1461-9563.2009.00437.x

Koven, C. D., Schuur, E. A. G., Schädel, C., Bohn, T. J., Burke, E. J., Chen, G., et al. (2015). A simplified, data-constrained approach to estimate the permafrost carbon-climate feedback. *Philosophical Transactions of Royal Society*, *373*, 20140423. https://doi.org/10.1098/rsta.2014.0423

Kruse, S., Gerdes, A., Kath, N. J., & Herzschuh, U. (2018). Implementing spatially explicit wind-driven seed and pollen dispersal in the individual-based larch simulation model: LAVESI-WIND 1.0. *Geoscientific Model Development*, *11*, 4451–4467. https://doi.org/10.5194/gmd-11-4451-2018

Kruse, S., Stuenzi, S. M., Boike, J., Langer, M., Gloy, J., & Herzschuh, U. (2022). Novel coupled permafrost-forest model revealing the interplay between permafrost, vegetation and climate across eastern Siberia. *Geoscientific Model Development*, *15*, 2395–2422. https://doi.org/10.5194/gmd-15-2395-2022

Kruse, S., Stuenzi, S. M., & Gloy, J. (2022). *LAVESI-CryoGrid v1.0*. https://doi.org/10.5281/ZENODO.5963455

Kruse, S., Wieczorek, M., Jeltsch, F., & Herzschuh, U. (2016). Treeline dynamics in Siberia under changing climates as inferred from an individual-based model for Larix. *Ecological Modelling*, *338*, 101–121. https://doi.org/10.1016/j.ecolmodel.2016.08.003

Langer, M., Westermann, S., Muster, S., Piel, K., & Boike, J. (2011). The surface energy balance of a polygonal tundra site in northern Siberia - Part 1: Spring to fall. *The Cryosphere*, *5*(2), 509–524. https://doi.org/10.5194/tc-5-151-2011

Li, X. Y., Jin, H. J., Wang, H. W., Marchenko, S. S., Shan, W., Luo, D. L., et al. (2021). Influences of forest fires on the permafrost environment: A review. *National Climate Center*, *12*(No. 1), 48–65. https://doi.org/10.1016/j.accre.2021.01.001

Liu, Y., Wang, Z., Sun, Q., Erb, A. M., Li, Z., Schaaf, C. B., et al. (2017). Evaluation of the VIIRS BRDF, Albedo and NBAR products suite and an assessment of continuity with the long term MODIS record. *Remote Sensing of Environment*, *201*, 256–274. https://doi.org/10.1016/j.rse.2017.09.020

Liu, Z. (2016). Effects of climate and fire on short-term vegetation recovery in the boreal larch forests of Northeastern China. *Scientific Reports*, *6*(1), 1–14. https://doi.org/10.1038/srep37572

Lodge, A. G., Dickinson, M. B., & Kavanagh, K. L. (2018). Xylem heating increases vulnerability to cavitation in longleaf pine. *Environmental Research Letters*, *13*(5), 055007. https://doi.org/10.1088/1748-9326/AABBE5

Loranty, M. M., Abbott, B. W., Blok, D., Douglas, T. A., Epstein, H. E., Forbes, B. C., et al. (2018). Reviews and syntheses: Changing ecosystem influences on soil thermal regimes in northern high-latitude permafrost regions. *Biogeosciences*, *15*, 5287–5313. https://doi.org/10.5194/bg-15-5287-2018

Loranty, M. M., Lieberman-Cribbin, W., Berner, L. T., Natali, S. M., Goetz, S. J., Alexander, H. D., & Kholodov, A. L. (2016). Spatial variation in vegetation productivity trends, fire disturbance, and soil carbon across arctic-boreal permafrost ecosystems. *Environmental Research Letters*, *11*(9), 095008. https://doi.org/10.1088/1748-9326/11/9/095008

Mamet, S. D., Brown, C. D., Trant, A. J., & Laroque, C. P. (2019). Shifting global Larix distributions: Northern expansion and southern retraction as species respond to changing climate. *Journal of Biogeography*, *46*(1), 30–44. https://doi.org/10.1111/JBI.13465

Maximov, T., Petrov, R., Iijima, Y., Hiyama, T., Ohta, T., Kotani, A., & Nakai, T. (2019). *Meteorological data at larch forest in eastern Siberia [Spasskaya Pad, 2016-2019]*, 1.00, Arctic Data archive System (ADS). Retrieved from https://ads.nipr.ac.jp/dataset/A20191107-009

Mekonnen, Z. A., Riley, W. J., Randerson, J. T., Grant, R. F., & Rogers, B. M. (2019). Expansion of high-latitude deciduous forests driven by interactions between climate warming and fire. *Nature Plants*, *5*(9), 952–958. https://doi.org/10.1038/s41477-019-0495-8

Meredith, M., Sommerkorn, M., Cassotta, S., Derksen, C., Ekaykin, A., Hollowed, A., et al. (2019). Polar Regions. In: IPCC Special Report on the Ocean and Cryosphere in a Changing Climate [H.-O. Pörtner, D.C. Roberts, V. Masson-Delmotte, P. Zhai, M. Tignor, E. Poloczanska, et al. (eds.)]. Cambridge University Press, (pp. 203–320). https://doi.org/10.1017/9781009157964.005.

Müller, W. A., Jungclaus, J. H., Mauritsen, T., Baehr, J., Bittner, M., Budich, R., et al. (2018). A higher-resolution version of the Max Planck Institute Earth system model (MPI-ESM1.2-HR). *Journal of Advances in Modeling Earth Systems*, *10*, 1383–1413. https://doi.org/10.1029/2017MS001217

Narita, D., Gavrilyeva, T., & Isaev, A. (2020). Impacts and management of forest fires in the republic of Sakha, Russia: A local perspective for a global problem. *Polar Science*, *27*, 100573. https://doi.org/10.1016/j.polar.2020.100573

Nitzbon, J., Langer, M., Westermann, S., Martin, L., Aas, K. S., & Boike, J. (2019). Pathways of ice-wedge degradation in polygonal tundra under different hydrological conditions. *The Cryosphere*, *13*(4), 1089–1123. https://doi.org/10.5194/tc-13-1089-2019

O'Donnell, J. A., Harden, J. W., McGuire, A. D., & Romanovsky, V. E. (2011). Exploring the sensitivity of soil carbon dynamics to climate change, fire disturbance and permafrost thaw in a black spruce ecosystem. *Biogeosciences*, *8*(5), 1367–1382. https://doi.org/10.5194/bg-8-1367-2011

Ohta, T., Hiyama, T., Tanaka, H., Kuwada, T., Maximov, T. C., Ohata, T., & Fukushima, Y. (2001). Seasonal variation in the energy and water exchanges above and below a larch forest in eastern Siberia. *Hydrological Processes*, *15*(8), 1459–1476. https://doi.org/10.1002/hyp.219

Oleson, K. W., Lead, D. M. L., Bonan, G. B., Drewniak, B., Huang, M., Koven, C. D., et al. (2013). *Technical description of version 4.5 of the community land model (CLM) (No. NCAR/TN-503 + STR)*. (Tech. Rep.) https://doi.org/10.5065/D6RR1W7M

Otoda, T., Doi, T., Sakamoto, K., Hirobe, M., Nachin, B., & Yoshikawa, K. (2013). Frequent fires may alter the future composition of the boreal forest in northern Mongolia. *Journal of Forest Research*, *18*(3), 246–255. https://doi.org/10.1007/s10310-012-0345-2

Painter, S. L., & Karra, S. (2014). Constitutive model for unfrozen water content in subfreezing unsaturated soils. *Vadose Zone Journal*, *13*(4), 1–8. https://doi.org/10.2136/vzj2013.04.0071

Pearson, R. G., Phillips, S. J., Loranty, M. M., Beck, P. S., Damoulas, T., Knight, S. J., & Goetz, S. J. (2013). Shifts in Arctic vegetation and associated feedbacks under climate change. *Nature Climate Change*, *3*(7), 673–677. https://doi.org/10.1038/nclimate1858

Peng, X., Zhang, T., Frauenfeld, O. W., Wang, S., Qiao, L., Du, R., & Mu, C. (2020). Northern hemisphere greening in association with warming permafrost. *Journal of Geophysical Research: Biogeosciences*, *125*(1), 1–20. https://doi.org/10.1029/2019JG005086

Petrov, M. I., Fedorov, A. N., Konstantinov, P. Y., & Argunov, R. N. (2022). Variability of permafrost and landscape conditions following forest fires in the central Yakutian taiga zone. *Land*, *11*(4), 496. Retrieved from https://doi.org/10.3390/LAND11040496

Ponomarev, E., Kharuk, V., & Ranson, K. (2016). Wildfires dynamics in Siberian larch forests. *Forests*, *7*(6), 125. Retrieved from https://doi.org/10.3390/f7060125

Randerson, J. T., Liu, H., Flanner, M. G., Chambers, S. D., Jin, Y., Hess, P. G., et al. (2006). The impact of boreal forest fire on climate warming. *Science*, *314*, 5802. Retrieved from https://doi.org/10.1126/science.1132075

Rey, D. M., Walvoord, M. A., Minsley, B. J., Ebel, B. A., Voss, C. I., & Singha, K. (2020). Wildfire-initiated talik development exceeds current thaw projections: Observations and models from Alaska's continuous permafrost zone. *Geophysical Research Letters*, *47*(15), e2020GL087565. https://doi.org/10.1029/2020GL087565

Rogers, B. M., Soja, A. J., Goulden, M. L., & Randerson, J. T. (2015). Influence of tree species on continental differences in boreal fires and climate feedbacks. *Nature Geoscience*, *8*(3), 228–234. https://doi.org/10.1038/ngeo2352

Romanovsky, V., Smith, S., Shiklomanov, N., Streletskiy, D., Isaksen, K., Kholodov, A., et al. (2017). Terrestrial permafrost in state of the climate in 2016. *Bulletin of the American Meteorological Society*, *98*(8), 147–149. https://doi.org/10.1175/2017BAMSStateoftheClimate.1

Sato, H., Kobayashi, H., Beer, C., & Fedorov, A. (2020). Simulating interactions between topography, permafrost, and vegetation in Siberian larch forest. *Environmental Research Letters*, *15*, 095006. https://doi.org/10.1088/1748-9326/ab9be4

Sato, H., Kobayashi, H., & Delbart, N. (2010). Simulation study of the vegetation structure and function in eastern Siberian larch forests using the individual-based vegetation model SEIB-DGVM. *Forest Ecology and Management*, *259*(3), 301–311. https://doi.org/10.1016/j.foreco.2009.10.019

Sato, H., Kobayashi, H., Iwahana, G., & Ohta, T. (2016). Endurance of larch forest ecosystems in eastern Siberia under warming trends. *Ecology and Evolution*, *6*(16), 5690–5704. https://doi.org/10.1002/ece3.2285

Schulze, E.-D., Wirth, C., Mollicone, D., Von, N., Upke, L., Ziegler, W., et al. (2012). Factors promoting larch dominance in central Siberia: Fire versus growth performance and implications for carbon dynamics at the boundary of evergreen and deciduous conifers. *Biogeosciences*, *9*, 1405–1421. https://doi.org/10.5194/bg-9-1405-2012

Shuman, J. K., Foster, A. C., Shugart, H. H., Hoffman-Hall, A., Krylov, A., Loboda, T., et al. (2017). Fire disturbance and climate change: Implications for Russian forests. *Environmental Research Letters*, *12*(3), 035003. https://doi.org/10.1088/1748-9326/AA5EED

Shuman, J. K., Shugart, H. H., & O'Halloran, T. L. (2011). Sensitivity of Siberian larch forests to climate change. *Global Change Biology*, *17*(7), 2370–2384. https://doi.org/10.1111/j.1365-2486.2011.02417.x

Shuman, J. K., Tchebakova, N. M., Parfenova, E. I., Soja, A. J., Shugart, H. H., Ershov, D., & Holcomb, K. (2014). Forest forecasting with vegetation models across Russia. *Canadian Journal of Forest Research*, *45*(2), 175–184. https://doi.org/10.1139/cjfr-2014-0138

Shvidenko, A. Z., & Nilsson, S. (2000). Extent, distribution, and ecological role of fire in Russian forests. In *Fire, climate change, and carbon cycling in the boreal forest* (pp. 132–150). Springer. https://doi.org/10.1007/978-0-387-21629-4_8

Simmons, A., Uppala, S., Dee, D., & Kobayashi, S. (2007). *ERA-interim: New ECMWF Reanalysis 20 Products from 1989 Onwards (Tech. Rep.). ECMWF Newsletter* (Vol. 110). https://doi.org/10.21957/pocnex23c6

Soja, A. J., Cofer, W. R., Shugart, H. H., Sukhinin, A. I., Stackhouse, P. W., McRae, D. J., & Conard, S. G. (2004). Estimating fire emissions and disparities in boreal Siberia (1998-2002). *Journal of Geophysical Research: Atmospheres*, *109*(14), D14S06. https://doi.org/10.1029/2004JD004570

Stuenzi, S. M., Boike, J., Cable, W., Herzschuh, U., Kruse, S., Pestryakova, L. A., et al. (2021). Variability of the surface energy balance in permafrost-underlain boreal forest. *Biogeosciences*, *18*, 343–365. https://doi.org/10.5194/bg-18-343-2021

Stuenzi, S. M., Boike, J., Gädeke, A., Herzschuh, U., Kruse, S., Pestryakova, L. A., et al. (2021). Sensitivity of ecosystem-protected permafrost under changing boreal forest structures. *Environmental Research Letters*, *16*(8), 084045. https://doi.org/10.1088/1748-9326/AC153D

Stuenzi, S. M., Kruse, S., Boike, J., Herzschuh, U., Westermann, S., & Langer, M. (2021). *Coupled multilayer canopy-permafrost model (CryoGrid) for the use with an individual-based larch vegetation simulator (LAVESI)*. https://doi.org/10.5281/ZENODO.5119987

Stuenzi, S. M., & Schaepman Strub, G. (2020). Vegetation trajectories and shortwave radiative forcing following boreal forest disturbance in eastern Siberia. *Journal of Geophysical Research: Biogeosciences*, *125*, e2019JG005395. https://doi.org/10.1029/2019jg005395

Sugimoto, A., Yanagisawa, N., Naito, D., Fujita, N., & Maximov, T. C. (2002). Importance of permafrost as a source of water for plants in east Siberian taiga. *Ecological Research*, *17*(4), 493–503. https://doi.org/10.1046/j.1440-1703.2002.00506.x

Takahashi, K. (2006). Future perspective of forest management in a Siberian permafrost area. *Symptom of environmental change in Siberian permafrost*, (pp. 163–170). Retrieved from http://www.agr.hokudai.ac.jp/env/ctc_siberia/pdf_book/18_Takahashi.pdf

Tanaka, H., Hiyama, T., Kobayashi, N., Yabuki, H., Ishii, Y., Desyatkin, R. V., et al. (2008). Energy balance and its closure over a young larch forest in eastern Siberia. *Agricultural and Forest Meteorology*, *148*(12), 1954–1967. https://doi.org/10.1016/j.agrformet.2008.05.006

Tchebakova, N. M., Parfenova, E., & Soja, A. J. (2009). The effects of climate, permafrost and fire on vegetation change in Siberia in a changing climate. *Environmental Research Letters*, *4*(4), 045013. https://doi.org/10.1088/1748-9326/4/4/045013

Tchebakova, N. M., Parfenova, E. I., Korets, M. A., & Conard, S. G. (2016). Potential change in forest types and stand heights in central Siberia in a warming climate Potential change in forest types and stand heights in central Siberia in a warming climate. *Environmental Research Letters*, *11*, 35016. https://doi.org/10.1088/1748-9326/11/3/035016

Ulrich, M., Matthes, H., Schirrmeister, L., Schütze, J., Park, H., Iijima, Y., & Fedorov, A. N. (2017). Differences in behavior and distribution of permafrost-related lakes in Central Yakutia and their response to climatic drivers. *Water Resources Research*, *53*(2), 1167–1188. https://doi.org/10.1002/2016WR019267

Varner, J. M., Hood, S. M., Aubrey, D. P., Yedinak, K., Hiers, J. K., Jolly, W. M., et al. (2021). Tree crown injury from wildland fires: Causes, measurement and ecological and physiological consequences. *New Phytologist*, *231*(5), 1676–1685. https://doi.org/10.1111/NPH.17539

Vionnet, V., Brun, E., Morin, S., Boone, A., Faroux, S., Le Moigne, P., et al. (2012). The detailed snowpack scheme Crocus and its implementation in SURFEX v7.2. *Geoscientific Model Development*, *5*, 773–791. https://doi.org/10.5194/gmd-5-773-2012

Westermann, S., Langer, M., Boike, J., Heikenfeld, M., Peter, M., Etzelmüller, B., & Krinner, G. (2016). Simulating the thermal regime and thaw processes of ice-rich permafrost ground with the land-surface model CryoGrid 3. *Geoscientific Model Development*, *9*(2), 523–546. https://doi.org/10.5194/gmd-9-523-2016

Wirth, C. (2005). Fire Regime and Tree Diversity in Boreal Forests: Implications for the Carbon Cycle. In: Scherer-Lorenzen M., Körner C., Schulze ED. (eds), *Forest Diversity and Function. Ecological Studies* (vol 176). Springer. https://doi.org/10.1007/3-540-26599-6_15

Yershov, E. (2004). In P. J.Williams (Ed.), *General Geocryology*. Cambridge University Press. Retrieved from https://doi.org/10.1017/CBO9780511564505

Yi, S., Woo, M.-k., & Arain, M. A. (2007). Impacts of peat and vegetation on permafrost degradation under climate warming. *Geophysical Research Letters*, *34*(16), L16504. https://doi.org/10.1029/2007GL030550

Yoshikawa, K., Bolton, W. R., Romanovsky, V. E., Fukuda, M., & Hinzman, L. D. (2002). Impacts of wildfire on the permafrost in the boreal forests of Interior Alaska. *Journal of Geophysical Research*, *107*, FFR4-1–FFR4-11. https://doi.org/10.1029/2001JD000438

Zhang, N., Shugart, H. H., & Yan, X. (2009). Simulating the effects of climate changes on Eastern Eurasia forests. *Climatic Change*, *95*(3–4), 341–361. https://doi.org/10.1007/s10584-009-9568-4

Zhang, N., Yasunari, T., & Ohta, T. (2011). Dynamics of the larch taiga-permafrost coupled system in Siberia under climate change. *Environmental Research Letters*, *6*(2), 024003. https://doi.org/10.1088/1748-9326/6/2/024003

Zweigel, R. B., Westermann, S., Nitzbon, J., Langer, M., Boike, J., Etzelmüller, B., & Schuler, T. V. (2021). Simulating snow redistribution and its effect on ground surface temperature at a high-Arctic site on Svalbard. *Journal of Geophysical Research: Earth Surface*, *126*(3), e2020JF005673. https://doi.org/10.1029/2020jf005673